

000 001 002 003 004 005 LESS IS MORE: UNDERTRAINING EXPERTS IMPROVES 006 MODEL UPCYCLING 007 008 009

010 **Anonymous authors**
011 Paper under double-blind review
012
013
014
015
016
017
018
019
020
021
022
023
024
025
026
027
028

ABSTRACT

029 Modern deep learning is increasingly characterized by the use of open-weight
030 foundation models that can be fine-tuned on specialized datasets. This has led
031 to a proliferation of expert models and adapters, often shared via platforms like
032 HuggingFace and AdapterHub. To leverage these resources, numerous model up-
033 cycling methods have emerged, enabling the reuse of fine-tuned models in multi-
034 task systems. A natural pipeline has thus formed to harness the benefits of transfer
035 learning and amortize sunk training costs: models are pre-trained on general data,
036 fine-tuned on specific tasks, and then upcycled into more general-purpose systems.
037 A prevailing assumption is that improvements at one stage of this pipeline propa-
038 gate downstream, leading to gains at subsequent steps. In this work, we challenge
039 that assumption by examining how expert fine-tuning affects model upcycling.
040 We show that long fine-tuning of experts that optimizes for their individual per-
041 formance leads to degraded merging performance, both for fully fine-tuned and
042 LoRA-adapted models, and to worse downstream results when LoRA adapters
043 are upcycled into MoE layers. We trace this degradation to the memorization of
044 a small set of difficult examples that dominate late fine-tuning steps. This causes
045 negative parameter interference and encodes knowledge that is forgotten during
046 merging. Finally, we demonstrate that task-dependent aggressive early stopping
047 strategies can significantly improve upcycling performance.
048
049

1 INTRODUCTION

050 The rise of open-weight foundation models, such as CLIP (Radford et al., 2021; Ilharco et al., 2021),
051 T5 (Raffel et al., 2020) and the more recent Gemma (Team, 2025), Llama (Grattafiori et al., 2024)
052 and DeepSeek (DeepSeek-AI, 2024), has caused a paradigm shift in the field of machine learning.
053 Instead of training a model from scratch as was previously the norm, it is now increasingly common
054 for practitioners and researchers alike to start with a pre-trained foundation model and then fine-tune
055 it on a task of interest (Stanford-CRFM, 2021). This approach leverages the benefits of transfer-
056 learning, leading to performance and robustness gains. The proposal of multiple parameter-efficient
057 fine-tuning (PEFT) methods (Hu et al., 2022; Liu et al., 2022), which reduce the computational costs
058 of fine-tuning and limit catastrophic forgetting by only updating a subset of the model parameters,
059 further enables this approach. This has lead to a proliferation of different versions of these founda-
060 tion models and of PEFT adapters, fine-tuned on a variety of downstream tasks, which are openly
061 accessible on public model repositories such as Hugging Face (Wolf et al., 2019) and Adapter Hub
062 (Pfeiffer et al., 2020).

063 Model *upcycling*, the practice of reusing existing models to create new, more capable deep learning
064 systems (Zhang et al., 2024; He et al., 2024), capitalizes on this proliferation of fine-tuned models
065 and adapters. Two upcycling strategies stand out: *model merging*, and *model MoErging*. Model
066 merging methods combine multiple fine-tuned versions of the same foundational model into one,
067 preserving the size and therefore the computational and memory requirements of the original pre-
068 trained model while infusing it with multiple new capabilities (Matena & Raffel, 2022; Jin et al.,
069 2023; Ilharco et al., 2023; Yadav et al., 2023; Yu et al., 2024; Davari & Belilovsky, 2024). The
070 advent of model merging techniques and open-source libraries for merging (Kandpal et al., 2023;
071 Goddard et al., 2024) has had an important impact on the deep learning community, providing a
072 simple, training-free way to create better models from already existing checkpoints and adapters.
073

054 In the past year, many of the top performing models on HuggingFace’s Open LLM Leaderboard
 055 (Beeching et al., 2023) have resulted from the merging of fine-tuned checkpoints (Yu et al., 2024).
 056

057 Model MoErging (Yadav et al., 2024) similarly combines multiple adapted experts, but instead of
 058 fusing the parameters directly, MoErging approaches such as Ostapenko et al. (2024); Muqeeth et al.
 059 (2024) combine adapters into modular, mixture-of-experts (MoE) type layers (Shazeer et al., 2017)
 060 expanding the model’s size and capabilities. A routing mechanism determines which input, or part
 061 of the input, gets processed by which expert modules. For this upcycling strategy further training is
 062 often required to let the router and expert adapters learn how to interact with one another.
 063

064 A natural pipeline has therefore emerged to leverage the benefits of transfer-learning and amortize
 065 past sunk training costs: large models are *pre-trained* in an unsupervised fashion on large amounts
 066 of general, unlabeled data; these foundational models are then *fine-tuned*, potentially using PEFT
 067 techniques, on specialized datasets or tasks; finally these fine-tuned expert checkpoints or adapters
 068 are *upcycled* and combined to create more capable, often multi-task models.
 069

070 A common assumption is that *increased performance at one stage of this pipeline will propagate*
 071 *downstream*. In other words, a stronger pre-trained model should yield a stronger fine-tuned model,
 072 and similarly, stronger fine-tuned experts should produce a stronger merged / MoErged model. We
 073 challenge this assumption in this work by studying the following questions: *How does expert training*
 074 *affect upcycling?* and *Do all capabilities and knowledge transfer equally well?*
 075

076 We find that long fine-tuning that optimizes for expert performance can substantially hurt model
 077 upcycling, a phenomenon to which we refer as “overtraining” in the context of this paper. While
 078 overtrained experts might be better on their respective fine-tuning tasks, they lead to worse performance
 079 when merged or when used as initializations for model MoErging. We validate this phenomenon across diverse settings, including merging fully fine-tuned and PEFT models, performing
 080 MoErging with LoRA adapters, in both vision and language domains and across different model
 081 families and sizes. We use tools from the data difficulty literature to link prolonged training to the
 082 memorization of hard examples. This memorization causes negative parameter interference, leading
 083 to hard examples being overwhelmingly forgotten during merging, while easy examples remain
 084 correctly classified. While some recent work has hinted that undertraining experts can benefit merging
 085 performance (Pari et al., 2024; Zhou et al., 2025), our work provides a systematic analysis of this
 086 phenomenon, and demonstrates how simple early stopping strategies can significantly improve the
 087 efficacy of existing merging and MoErging techniques. Our research introduces a critical new dimension
 088 to model upcycling, showing how careful expert training, and targeted checkpoint release
 089 can unlock improved performance.
 090

091 Concretely, our contributions are the following:
 092

- 093 • We show that overtraining full fine-tuned (FFT) models produces sub-optimal merges (Section
 094 3.1), and that the negative impact is even stronger when using LoRA adapters for
 095 parameter-efficient fine-tuning (Section 3.2);
 096 • We explain this phenomenon through the lens of data difficulty in Section 4, showing that later
 097 training steps are dominated by the memorization of a small fraction of difficult examples,
 098 which are predominantly forgotten during merging due to negative parameter interference.
 099 • We show that for model MoErging, overtraining the constituent experts leads to lower final
 100 accuracy after further multi-task training of the modular model (Section 3.3).
 101 • We show that task-dependent expert training duration can further improve upcycling perfor-
 102 mance. We propose early stopping as a general principle to encourage expert undertraining.
 103 Our early stopping strategies effectively adapt training duration per task and can recover opti-
 104 mal upcycling accuracy (Section 5).
 105

106 2 PRELIMINARIES AND METHODOLOGY

107 2.1 MODEL MERGING

108 Model merging has recently gained a lot of popularity as a means to combine the abilities of multiple
 109 fine-tuned versions of the same pre-trained model into one, preserving the model architecture and
 110 size (Yang et al., 2024). Formally, a model merging method, Merge , takes the parameters θ_0 of
 111 the pre-trained foundation model, and parameters $\{\theta_t\}_{t \in \mathcal{T}}$ of the multiple *experts*, which are fine-
 112 tuned models on each task t from a set \mathcal{T} , and outputs the parameters of the merged model $\bar{\theta} =$
 113 $\text{Merge}(\theta_0, \{\theta_t\}_{t \in \mathcal{T}})$. A simple example of this combination step is averaging the different fine-

108 tuned models’ parameters:

$$\bar{\theta} = \frac{1}{|\mathcal{T}|} \sum_{t \in \mathcal{T}} \theta_t. \quad (1)$$

111 Merging methods are generally motivated by the observation that fine-tuned models exhibit *linear*
 112 *mode connectivity*: their loss minima are connected by low-loss linear paths in parameter space
 113 (Frankle et al., 2020; Sharma et al., 2024). This property typically emerges because fine-tuned mod-
 114 els share substantial portions of their training trajectories (Frankle et al., 2020; Neyshabur et al.,
 115 2020), and is therefore a key reason merging is expected to be feasible. Nonetheless, a common
 116 challenge in model merging is the observed performance degradation of the merged model $\bar{\theta}$ on
 117 individual tasks $t \in \mathcal{T}$, relative to the original fine-tuned model θ_t . This phenomenon has been
 118 coined “interference”, and a plethora of merging methods have been proposed to reduce interfer-
 119 ence when merging models and to preserve as much of the accuracy of the expert models as possible
 120 (Matena & Raffel, 2022; Jin et al., 2023; Yadav et al., 2023; Yu et al., 2024; Deep et al., 2024;
 121 Davari & Belilovsky, 2024). These methods have mainly focused on modifying the experts par-
 122 ameters $\{\theta_t\}_{t \in \mathcal{T}}$ or the respective *task vectors* $\{\tau_t\}_{t \in \mathcal{T}}$, where $\tau_t = \theta_t - \theta_0$, and / or changing the
 123 combination step. We consider 4 popular merging methods:

- **Average** simply averages the parameters of all fine-tuned models following Equation (1);
- **Task Arithmetic (TA)** (Ilharco et al., 2023) scales the sum of the task vectors by a tuned scalar
 λ , and adds it to the pre-trained model parameters, returning $\theta_0 + \lambda \sum_{t \in \mathcal{T}} \tau_t$;
- **TIES** (Yadav et al., 2023) prunes low magnitude parameters from each task vector, then only
 averages the remaining parameters if they have the same sign as the weighted majority;
- **DARE** (Yu et al., 2024) randomly prunes a fraction of each task vector parameters; the remain-
 ing parameters are rescaled based on the pruning fraction, and are combined as in TA.

131 We review other popular methods in Appendix A and detail our hyperparameter tuning procedure for
 132 merging in Appendix B. Prior works have primarily focused on deriving new techniques to reduce
 133 interference while assuming fixed, standard fine-tuning protocols. The role of the fine-tuning pro-
 134 cedure itself, particularly its duration, has received little attention, with some exceptions discussed in
 135 Section 6. Our work explicitly studies how expert training time affects mergeability.

2.2 MODEL MOERGING

138 Another popular class of upcycling strategies besides model merging are model MoErging tech-
 139 niques. MoErging methods aggregate multiple fine-tuned experts with the use of modular architec-
 140 tures, such as mixture-of-experts (MoE) layers (Shazeer et al., 2017), to build stronger deep learning
 141 systems. The large design space of these methods, paired with their effectiveness has led to the rapid
 142 development of many new methods in the recent past, with varying expert, router and application de-
 143 sign choices (Yadav et al., 2024; Huang et al., 2024; Ostapenko et al., 2024; Muqeeth et al., 2024). A
 144 key feature of MoErging approaches is modularity; multiple experts are considered simultaneously
 145 and a routing mechanism decides which input, or part of an input, is processed by which expert.

146 In this work we consider per-token and per-layer routing, following recent works which suggest
 147 this leads to better performance relative to other possible configurations (Ostapenko et al., 2024;
 148 Muqeeth et al., 2024). Concretely, let $\mathbf{W} \in \mathbb{R}^{d_{\text{out}} \times d_{\text{in}}}$, $b \in \mathbb{R}^{d_{\text{out}}}$ denote the weight matrix and
 149 bias of a pre-trained linear layer, whose original output is $\mathbf{W}x + b$. We assume the availability of
 150 a fine-tuned expert module $E_t(\cdot)$ for each target task $t \in \mathcal{T}$ and we replace the original linear layer
 151 with a MoE layer. A router π parameterized by matrix $R \in \mathbb{R}^{|\mathcal{T}| \times d_{\text{in}}}$ computes routing logits Rx
 152 and applies softmax $\sigma(\cdot)$ to obtain the routing probabilities. The outputs of the experts with top k
 153 highest probabilities are then computed and weight-averaged. The resulting MoE layer output is:

$$y = \mathbf{W}x + b + \frac{\sum_{t \in I_k(x)} \pi(x)_t E_t(x)}{\sum_{t \in I_k(x)} \pi(x)_t}, \quad (2)$$

157 where $I_k(x) = \{t \mid \pi(x)_t \in \text{top } k \text{ elements of } \pi(x)\}$. We use $k = 2$ for our experiments.

159 We consider the “multi-task” setting where we assume access to all the datasets the experts were
 160 trained on. After updating every linear layer of the pre-trained model with available adapters, we
 161 continue training the MoE-fied model on the multi-task mixture of data by freezing the original
 model parameters and only updating the router and the expert modules. Our MoErging setup is

162 closely related to Ostapenko et al. (2024), which combines LoRA experts into MoE layers and
 163 initializes routers using Arrow, but we additionally assume access to the training data and continue
 164 multi-task training. Notably, while prior work spans many routing and architectural designs, none
 165 study how expert overtraining affects downstream MoErging performance.
 166

167 2.3 LOW-RANK ADAPTATION

168 Modern foundation models have tens, if not hundreds, of billions of parameters, making full
 169 fine-tuning impractical on typical hardware (Grattafiori et al., 2024; DeepSeek-AI, 2024; Team,
 170 2025). Parameter-Efficient Fine-Tuning (PEFT) updates only a small subset of the parameters to
 171 ease the computational burden and curb catastrophic forgetting (Hu et al., 2022; Liu et al., 2022).
 172 Low-Rank Adaptation (LoRA) (Hu et al., 2022), has emerged as one of the most popular PEFT
 173 methods due to its simplicity and effectiveness. LoRA inserts two low-rank matrices \mathbf{A} and \mathbf{B} into
 174 selected linear layers of a model. If the input and output dimension at that layer are n_{in} and n_{out} ,
 175 LoRA uses a rank $r \ll \min(n_{in}, n_{out})$ to define matrices $\mathbf{A} \in \mathbb{R}^{r \times n_{in}}$ and $\mathbf{B} \in \mathbb{R}^{n_{out} \times r}$. The
 176 output of that layer then becomes $(\mathbf{Wx} + \mathbf{b}) + \frac{\alpha}{r} \mathbf{B} \mathbf{A} \mathbf{x}$ where α is a scaling hyperparameter. During
 177 fine-tuning, the original model is frozen and only the LoRA's \mathbf{A}, \mathbf{B} matrices are updated.
 178

179 **Merging LoRA adapters** At each layer, the weight update induced by LoRA is exactly
 180 $\Delta W = W_{\text{fine-tuned}} - W_{\text{pre-trained}} = \frac{\alpha}{r} \mathbf{B} \mathbf{A}$. Consequently, standard merging techniques can be
 181 directly applied to LoRA-adapted models if the updates $\frac{\alpha}{r} \mathbf{B} \mathbf{A}$ are added to the pre-trained weights
 182 or if they are directly used to compute the task vectors. Merging the LoRA \mathbf{A} and \mathbf{B} matrices
 183 separately is not recommended since this can lead to mismatched representation spaces resulting in
 184 poor performance (Stoica et al., 2025). Nevertheless, recent work has observed that merging LoRA-
 185 adapted models is harder than merging FFT models (Tang et al., 2024a; Stoica et al., 2025), often
 186 leading to significant performance degradation.
 187

188 **Model MoErging with LoRA adapters** Using LoRA adapters for model MoErging is straight-
 189 forward, with each adapter being used to define one expert module in the MoE layer. Let \mathbf{A}_t and
 190 \mathbf{B}_t denote the LoRA low-rank matrices obtained from fine-tuning on task t , then we can define the
 191 expert modules in Equation (2) as $E_t(x) = \frac{\alpha}{r} \mathbf{B}_t \mathbf{A}_t x$ for each task of interest $t \in \mathcal{T}$.
 192

193 2.4 DATA DIFFICULTY

194 In this work, we use data difficulty scores to identify which knowledge is transferred during upcy-
 195 cling and to relate merging performance to training dynamics and memorization. Specifically, we
 196 use the EL2N score introduced by Paul et al. (2021) which measures the norm of the error vector,
 197 i.e. the predicted class probabilities minus the one-hot label encoding. For a training example x with
 198 one-hot label y , the EL2N score is defined as $\mathbb{E} \|p(\theta, x) - y\|_2$, where $p(\theta, x)$ denotes the model's
 199 predicted class probabilities for x under parameters θ .
 200

201 Prior work has examined how individual data points influence neural network training dynamics and
 202 properties such as generalization, memorization, and privacy, leading to the development of various
 203 data difficulty scores (Kwok et al., 2024). These scores aim to quantify an intrinsic characteristic of
 204 the data, namely *data difficulty*, which captures how easy or hard individual examples are to learn.
 205 Easy examples typically exhibit common, easily learnable features, whereas hard examples often
 206 possess idiosyncratic structure or even noisy labels. Such scores have been successfully used for
 207 data pruning, with past work showing that large fractions of easy examples can be removed with
 208 little effect on performance, while pruning a small fraction of the hardest examples can improve
 209 generalization by eliminating outliers with uncommon features (Toneva et al., 2019) or mislabeled
 210 data (Paul et al., 2021). Moreover, Sorscher et al. (2022) showed that appropriate data pruning can
 211 yield better-than-power-law error scaling with dataset size.
 212

213 A natural relationship exists between data difficulty and deep learning generalization and memo-
 214 rization. For instance, Sorscher et al. (2022) found a 0.78 Spearman rank correlation between EL2N
 215 scores (Paul et al., 2021) and the memorization score presented by Feldman & Zhang (2020). These
 216 observations suggest that correctly classifying difficult examples often requires memorization, and
 217 that a certain degree of memorization is therefore necessary for achieving near-optimal generaliza-
 218 tion. This relationship between memorization and generalization has been further substantiated with
 219 theoretical results in simpler settings (Attias et al., 2024; Feldman, 2020).
 220

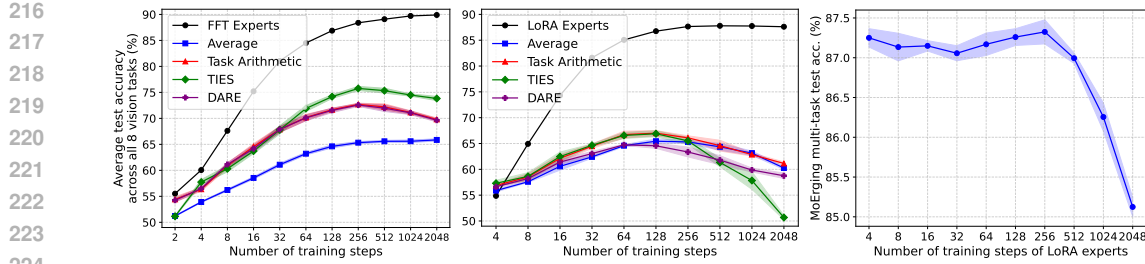


Figure 1: Average test accuracy across the 8 vision classification tasks for merged and MoErged ViT-B-32 experts. **Left:** merging fully fine-tuned experts, we plot the average accuracy of the expert models evaluated on their respective tasks as well as merging accuracies for multiple methods; **Center:** merging LoRA-adapted experts; **Right:** final multi-task accuracy of MoE-fied models vs. LoRA training steps used for initialization. Shaded regions show mean \pm std over 3 random seeds.

2.5 MODELS AND DATASETS

Vision domain We evaluate merging performance in a standard vision benchmark setting using the official codebase from Ilharco et al. (2023): a CLIP (Radford et al., 2021) pre-trained ViT-B-32 model (Dosovitskiy et al., 2021) is fine-tuned on 8 image classification tasks: Cars (Krause et al., 2013), DTD (Cimpoi et al., 2014), EuroSAT (Helber et al., 2019), GTSRB (Stallkamp et al., 2012), MNIST (Deng, 2012), RESISC45 (Cheng et al., 2017), SUN397 (Xiao et al., 2010) and SVHN (Netzer et al., 2011). The fine-tuning is done with a batch size of 128, the AdamW optimizer (Loshchilov & Hutter, 2019; Paszke et al., 2019) and a learning rate of 1e-5. We use a learning-rate scheduler with linear warm-up for the first 10% of training, followed by cosine annealing. When evaluating merged models, we use the corresponding frozen classification head for each task.

Language domain For our natural language processing (NLP) experiments, we adopt the setting of the TIES paper (Yadav et al., 2023) and use their released code. We use pre-trained T5-Base models (Raffel et al., 2020) which we fine-tune on 7 tasks: QASC (Khot et al., 2020), WikiQA (Yang et al., 2015) and QuaRTz (Tafjord et al., 2019) for question answering; PAWS (Zhang et al., 2019) for paraphrase identification; Story Cloze (Sharma et al., 2018) for sentence completion and Winogrande (Sakaguchi et al., 2020) and WSC (Levesque et al., 2012) for coreference resolution. We use the AdamW (Loshchilov & Hutter, 2019) optimizer with a batch size of 256, a constant lr of 0.0001 and no weight decay. bfloat16 mixed precision training is used to reduce GPU utilization.

Evaluation For all our experiments we report the raw, un-normalized test accuracy averaged across the multiple considered tasks. We chose not to use the popular *normalized accuracy* metric because the set of experts being merged here differs across experiments, which also changes the normalization factor and makes comparisons inconsistent. A more detailed justification is provided in Appendix C. Our experiments are ran using the PyTorch (Paszke et al., 2019) and HuggingFace (Wolf et al., 2019) open source machine learning frameworks on an Nvidia Quadro RTX 8000 GPU with 48GB of memory.

3 LONGER FINE-TUNING HURTS MODEL UPCYCLING

In this section, we present results challenging the common assumption that better fine-tuned models lead to better upcycling results. We show that overtrained experts lead to worse merged models for both FFT and LoRA, as well as lower accuracy when used to initialize MoErging methods.

3.1 MERGING FULLY FINE-TUNED MODELS

While a multitude of model merging methods have been proposed, the influence of the fine-tuning procedure itself on merging remains understudied. Most prior works have used similar fine-tuning protocols, typically training for a fixed 2000 steps in the vision setting described in Section 2.5. Instead of proposing yet another model merging method, we take a look at how the number of training iterations affects merging. We fine-tune our vision and NLP models for varying number of training steps $s \in \{2, 4, 8, 16, 32, 64, 128, 256, 512, 1024, 2048\}$ on every considered dataset. Each merge combines either 8 vision or 7 NLP experts (one per task) all trained for the same duration.

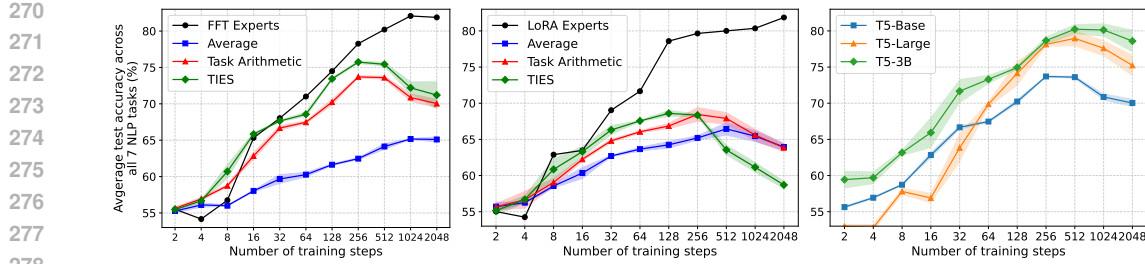


Figure 2: Average test accuracy across all 7 NLP tasks for fully fine-tuned (**left**) and LoRA-adapted (**center**) T5-Base models. We plot the average accuracy of the expert models evaluated on their respective tasks as well as merging accuracies for multiple methods. **Right:** Task Arithmetic merging accuracy for different T5 model sizes. Shaded regions show $\text{mean} \pm \text{std}$ over 3 random seeds.

Undertrained experts result in better merging Figure 1 (left) shows that, except for Average, all methods achieve better merging performance when the ViT experts are trained for just 256 training steps, only $\sim 1/8$ of the commonly used 2000. TA, TIES, and DARE yield models with $\sim 3\%$ higher accuracy at 256 steps compared to 2048, a gain comparable to the 3.4% gap between TA and the more sophisticated TIES at 2048 steps. The same conclusions hold in the NLP setting (Figure 2 left), with both TA and TIES peaking around 256–512 training steps. Further training leads to a drop in merging performance of over 3% for both merging methods. Notably, merging undertrained experts with TA outperforms merging experts trained for longer with TIES. Average is the only method that seems to benefit from training the experts longer, but it consistently underperforms overall. Moreover, TA, TIES, and DARE show similar trends across training durations, suggesting that training length itself, rather than the merging method, plays a key role in merging performance.

Better experts do not necessarily lead to better merging The black lines in the left and central panels of Figures 1 and 2 show the average accuracy of the expert models on their respective fine-tuning tasks. In both the vision and NLP settings, we observe that higher expert accuracy does not necessarily translate into better merging performance. In the vision setting, expert models trained for 256 steps achieve an average accuracy of 88.4%, which is 1.6% lower than at 2048 steps (90.0%). Nevertheless, merging after 256 steps yields models with approximately 3% higher accuracy than merging after 2048 steps. The discrepancy is even more pronounced in the NLP setting. Expert accuracy improves from 78.2% at 256 steps to 82.4% at 1024 steps, a 4% gain, yet the merging accuracy of TA and TIES drops by around 3% over the same interval. We provide a per-task breakdown of these results in Appendix D and further experiments with ViT-L-14 and BERT models in Appendix E. The same “overtraining degrades upcycling” phenomenon can be generally observed.

Effect of model scale In the right panel of Figure 2, we compare Task Arithmetic merging accuracy across different model sizes in the T5 family: T5-Base (220M parameters), T5-Large (770M), and T5-3B (3B). We observe that the same trend persists across scales: upcycling performance peaks at an intermediate number of training steps before degrading with longer fine-tuning. Additional merging results are provided in Appendix F.

3.2 MERGING LORA ADAPTERS

We now extend our previous results to the highly relevant setting of merging LoRA adapters. We find that long training of LoRA experts hurts merging performance even more than in the FFT case. We add LoRA adapters at every linear layer of the original ViT-B-32 and T5-Base models. We use LoRA rank $r = 8$, scaling parameter $\alpha = 32$ and learning rates 1e-4 and 5e-4 for the ViT and T5 models respectively. We train the LoRAs for different number of steps s to evaluate the impact of training duration on accuracy and mergeability. The parameters of the base model are kept frozen.

Overtraining severely impairs LoRA merging The center panels of Figures 1 and 2 show expert and merging accuracies for our vision and NLP LoRA models, respectively. For the ViT models, merging performance peaks at 128 training steps (64 for DARE), with accuracies ranging from 65–67% across all methods. Although further training improves expert accuracy by about 1%, it significantly degrades merging performance, with accuracy drops of 5–6% for Average, TA, and DARE, and nearly 17% for TIES. In the NLP setting, different methods reach peak merging performance at different training durations: 512 steps for Average (66.5%), 256 for TA (68.5%), and 128

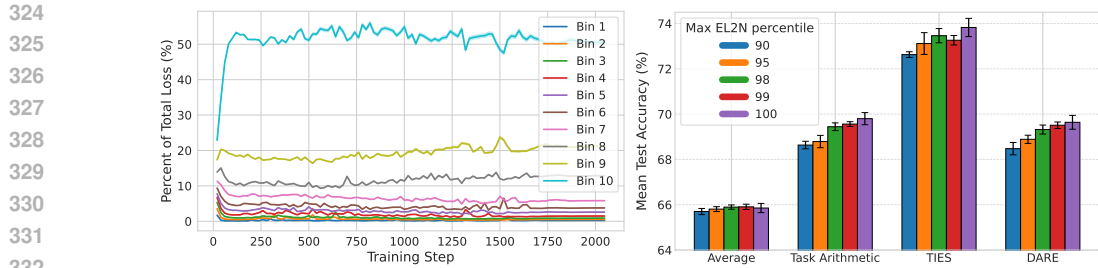


Figure 3: **Left:** Percentage of total loss for examples in different data difficulty bins. Bin 1 represents 10% easiest examples (lowest EL2N scores), bin 10 represents 10% hardest examples (highest EL2N scores). Mean across all 8 vision datasets shown. **Right:** Merging accuracy for experts trained without the hardest examples. Experts are trained on data with EL2N scores from percentile 0 to varying max percentiles in {90, 95, 98, 99, 100}.

for TIES (68.6%). Expert models, however, continue to improve, reaching an average accuracy of 81.9% at 2048 steps. Despite this, merging at 2048 steps harms performance, with drops of 2.5%, 4.6%, and 9.9% for Average, TA, and TIES, respectively. In Appendix G, we examine the impact of LoRA rank and show that higher ranks lead to smaller performance degradations when merging.

3.3 MODEL MOERGING WITH LORA EXPERTS

We next analyze how the performance of MoE-fied models, initialized with LoRA experts, is affected by the training time of these experts. We use the LoRA adapters obtained in Section 3.2 with different number of training steps to initialize our MoE experts, one LoRA for each task. The routing mechanism is initialized using Arrow (Ostapenko et al., 2024), where the weight vector associated with each expert is the first right-singular vector of the BA matrix multiplication. These vectors are assumed to determine the direction of most variance induced by expert E_t for $t \in \mathcal{T}$ in the space of hidden states induced by data from task t .

We create one MoE-fied model for each number of steps s , i.e. for each different model we initialize the MoE layers with the expert LoRAs for each task, all trained for s steps. Once the MoE-fied model has been initialized using the fine-tuned LoRAs, we further train the routing mechanism and the LoRA experts in a multi-task fashion for 4000 steps with a peak learning rate of 1e-5, with the base parameters frozen. We report the final, multi-task, accuracies over the 8 classification tasks in the right panel of Figure 1.

We observe that the MoE-fied models initialized with overtrained LoRA experts reach about 2% lower final multi-task accuracy than the models initialized with experts trained for less. Even expert LoRAs trained for as little as 4 steps on their respective tasks reach a higher final multi-task accuracy than those overtrained. We conclude that overtraining experts can hurt downstream MoErging.

4 WHY IS UNDERTRAINING BENEFICIAL FOR MERGING?

In this section we use tools from the data difficulty literature to explain why undertraining is beneficial for model merging. This allows us to make a series of empirical observations linking prolonged training to the memorization of hard examples and to increased parameter interference.

For all the training examples from the 8 considered image classification tasks we compute the EL2N data difficulty scores early in fine-tuning, after only 32 steps, across 10 different seeds (different models than the ones we merge). We note that despite being computed early in training, the EL2N scores aim to estimate an intrinsic characteristic of the data, independent of model training. To facilitate analysis, we group the training examples into 10 bins according to their EL2N scores, the 10% of examples with the lowest EL2N scores (the easiest examples) are in bin 1 and so on.

Observation 1: Later training stages are driven by the memorization of hard examples. In the left panel of Figure 3 we show the relative loss of the training examples during training. We observe that easy examples, which have more common features, are learned very early in training. **The remaining of training is driven largely by the loss of the difficult examples**, with the top 10% of hardest examples accounting for over 50% of the total loss after the first 100 steps. In Appendix H

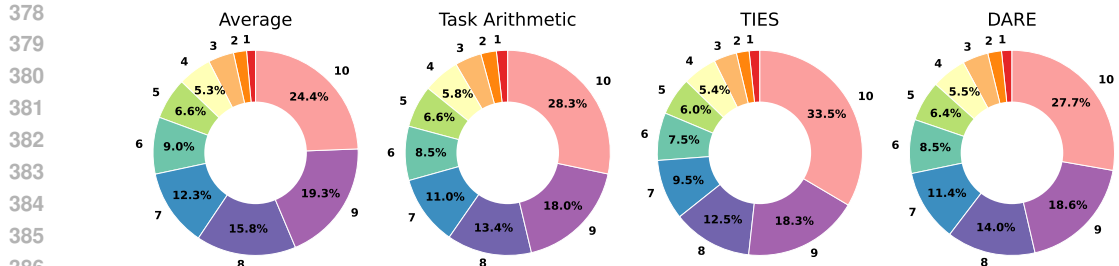


Figure 4: Proportion of forgotten examples in each data difficulty bin for three different model merging methods. Bin 1 represents 10% easiest examples (lowest EL2N scores), bin 10 represents 10% hardest examples (highest EL2N scores). Hard examples are overwhelmingly forgotten when merging with all methods, with the 30% hardest examples representing over 50% of forgotten examples.

we quantify memorization of examples in each data difficulty bin using three metrics: *change in margin* (gap between true class probability and maximum probability among other classes), *change in loss*, and *predictive distribution shift* (L1 norm of the difference between predicted probabilities). Comparing ViT-B-32 models trained for 256 and 2048 steps, all metrics show changes of orders of magnitude larger for the hardest examples (bin 10) than for the easiest (bin 1), despite only modest accuracy gains on the test set (1.6% on average) and on the training set (4%). This suggests that **memorization of hard examples occurs during the later stages of training**.

Observation 2: Later training stages result in idiosyncratic parameter updates causing increases in parameter interference. As discussed in Section 2.4, hard examples represent outliers with uncommon features or noisy labels. Therefore, it stands to reason that the memorization of such examples would also yield idiosyncratic parameter updates that don't generalize across tasks. In Appendix I we estimate the amount of parameter interference between the task vectors obtained with various training durations using four different metrics: *sign conflict percentage*, *parameter overlap percentage*, *magnitude ratio* and *per-parameter variance*. All of these parameter interference scores increase with training duration, confirming that **longer training yields idiosyncratic parameter updates leading to more parameter interference**. Since parameter interference is a well accepted explanation to the performance degradation observed when merging (Yadav et al., 2023), **this directly explains our main observation that longer training negatively impacts model merging**.

To directly link these parameter updates to the memorization of hard examples, we take a look at which examples are *forgotten* during merging, i.e. training examples correctly classified by the expert models but incorrectly classified after merging. Figure 4 shows that hard examples are disproportionately forgotten during merging, with over 50% of forgotten data points in the top 30% in terms of data difficulty. This confirms that parameter updates from prolonged training are idiosyncratic and driven by memorization of hard examples, and that merging destroys some of these learned features due to parameter interference.

Observation 3: Difficult examples are still necessary for good upcycling generalization. Inspired by work showing that removing difficult examples from training can aid generalization (Toneva et al., 2019; Paul et al., 2021), we investigate how this affects merging performance. We remove the top 1, 2, 5, or 10% most difficult examples from training and report merging results in the right panel of Figure 3. However, we find that the best merging results are achieved when all data is used and that removing difficult examples consistently hurts performance. This expands upon past work showing that some memorization is necessary for close-to-optimal generalization (Feldman, 2020; Feldman & Zhang, 2020; Attias et al., 2024) by demonstrating that **some amount of memorization is also necessary for close-to-optimal merging performance**.

5 AGGRESSIVE EARLY STOPPING IMPROVES UPCYCLING RESULTS

Our core finding that overtraining experts harms upcycling performance naturally motivates the use of early stopping to mitigate this effect. We hypothesize that early stopping during fine-tuning will yield stronger upcycling results, as it both shortens training duration and automatically adapts the stopping time for each task. In this section we investigate this hypothesis and find that upcycling can indeed be improved by early stopping, even when expert-level performance is lower. Our goal

432 Table 1: Experts and merging accuracy (%) for the overtrained, optimal and early stopped ViT-B
 433 experts. Mean and standard deviation across 3 random seeds shown.

| | Experts | Average | Task Arithmetic | TIES | DARE |
|----------------------|----------------|-----------------------|----------------------|----------------------|----------------------|
| FFT 2048 steps | 89.9 \pm 0.1 | 65.9 \pm 0.2 | 69.8 \pm 0.27 | 73.8 \pm 0.4 | 69.6 \pm 0.3 |
| FFT best (# steps) | - | 65.9 \pm 0.2 (2048) | 72.7 \pm 0.2 (256) | 75.8 \pm 0.4 (256) | 72.6 \pm 0.3 (256) |
| FFT early stop | 87.9 \pm 0.2 | 64.5 \pm 0.1 | 72.6 \pm 0.5 | 74.7 \pm 0.3 | 72.5 \pm 0.5 |
| LoRAs 2048 steps | 87.6 \pm 0.1 | 60.3 \pm 0.3 | 61.1 \pm 0.3 | 50.7 \pm 0.4 | 58.8 \pm 0.5 |
| LoRAs best (# steps) | - | 65.4 \pm 0.4 (128) | 67.0 \pm 0.5 (128) | 66.9 \pm 0.6 (128) | 64.7 \pm 0.1 (64) |
| LoRAs early stop | 87.9 \pm 0.1 | 65.6 \pm 0.4 | 68.0 \pm 0.8 | 67.1 \pm 0.6 | 65.3 \pm 0.3 |

442 here is not to establish the optimality of a single strategy, but to propose early stopping as a general
 443 principle for mitigating the negative effects of overtraining in upcycling and to introduce practical,
 444 automated variants that follows established best practices.

446 5.1 VISION SETTING — LINEAR WARM-UP AND ADAPTIVE DECAY

447 The learning rate scheduler used in Section 3 for ViT models, a linear warm-up followed by cosine
 448 decay, is a standard choice in vision training and recent merging work, where warm-up provides
 449 early stability and decay supports smooth convergence. Our early stopping strategy for these models
 450 retains this warm-up/decay structure while making it adaptive to the shorter, task-dependent training
 451 lengths induced by early stopping. We achieve this by pairing a 50-step linear warm-up phase with
 452 a “reduce learning rate on plateau” phase that gradually decreases the learning rate when validation
 453 accuracy stagnates. We compute the validation accuracy every 5 training steps and multiply the
 454 learning rate by 0.5 when it has not improved for 3 consecutive rounds. Once the learning rate
 455 falls below a threshold of 1e-7, training is stopped. We fine-tune FFT and LoRA models on the 8
 456 considered vision tasks using peak learning rates of 1e-5 and 1e-4 respectively. Pseudocode for this
 457 LR scheduler and early stopping strategy is provided in Appendix J.

458 In Table 1 we compare the merging of early stopped experts to two baselines from Section 3: merging
 459 “overtrained” models trained for 2048 steps and merging the checkpoints that achieved the highest
 460 accuracy among all training durations (same duration across tasks). We see that the models
 461 trained using our simple task-dependent early stopping strategy yield merges that are better than
 462 those of overtrained models and as good, if not better, than the best merged experts obtained with a
 463 common stopping time even though the experts are on worse on their respective tasks. Early stop-
 464 ping seems to work especially well for LoRA adaptation, yielding results on average better than the
 465 best ones from Section 3.2.

466 We also use the early-stopped LoRAs to initialize
 467 MoE layers and continue training in a multi-task
 468 fashion, as in Section 3.3. As shown in Table 2, the
 469 MoErged models initialized with the early stop Lo-
 470 RAs achieve the same accuracy as the best LoRAs
 471 across all training steps.

Table 2: Early stopping MoErging results

| Expert initialization | Avg. accuracy |
|------------------------|----------------|
| 2048 steps LoRAs | 85.1 \pm 0.1 |
| Best LoRAs (256 steps) | 87.3 \pm 0.2 |
| Early stop LoRAs | 87.3 \pm 0.1 |

472 5.2 NLP SETTING — STOPPING WHEN VALIDATION ACCURACY PLATEAUS

473 Our T5 models from Section 3.1 were trained with a constant learning rate, making the design of
 474 the early stopping criterion straightforward: we evaluate accuracy on a held-out validation set every
 475 #steps batches and stop training whenever the validation accuracy fails to improve for #wait
 476 consecutive evaluations. The checkpoint with the highest validation accuracy is selected as the
 477 expert. We study two variants of this strategy: **v0**, with #steps=100 and #wait=5, and a more
 478 aggressive **v1**, with #steps=50 and #wait=3. Results are presented in Table 3.

479 Experts obtained with v0 match the performance of models trained for 1024 or 2048 steps, while
 480 v1 yields slightly lower accuracy. Importantly, both strategies achieve these results with far fewer
 481 training iterations, on average only 485 steps for v0 and 269 steps for v1. We also note high variance
 482 for the number of steps across tasks. Despite the reduced training time, the merging performance
 483 improves substantially. Task Arithmetic and TIES both benefit: across seeds, both early stopping
 484 strategies produce merges that are roughly 4% more accurate than merges from experts trained for
 485 1024 or 2048 steps. Moreover, the merging results for early stopped models are even superior to the
 486 best results from Section 3.1 where the single best stopping point is selected commonly for all tasks.
 487 Average merging is the only method which doesn’t seem to benefit from early stopping.

486 Table 3: Merging accuracy (%) and number of training steps for the overtrained, optimal and early
 487 stopped T5 experts. Mean and standard deviation across 3 random seeds shown.

| | # steps | Experts | Average | Task Arithmetic | TIES |
|--------------------|---------------|----------------|-----------------------|----------------------|----------------------|
| 490 1024 steps | 1024 | 82.4 \pm 0.3 | 65.2 \pm 0.1 | 70.9 \pm 0.6 | 72.2 \pm 1.0 |
| 491 2048 steps | 2048 | 82.0 \pm 0.5 | 65.0 \pm 0.4 | 70.1 \pm 0.7 | 72.2 \pm 1.4 |
| 492 Best (# steps) | – | – | 65.2 \pm 0.1 (1024) | 73.7 \pm 0.2 (256) | 75.7 \pm 0.2 (256) |
| 493 Early stop v0 | 485 \pm 350 | 82.3 \pm 0.6 | 63.4 \pm 0.4 | 75.0 \pm 0.3 | 76.9 \pm 0.5 |
| 494 Early stop v1 | 269 \pm 199 | 81.3 \pm 0.4 | 62.8 \pm 0.4 | 74.0 \pm 0.1 | 77.0 \pm 0.3 |

6 RELATED WORK

497 **Special fine-tuning procedures for better merging** Several recent works study how modifications
 498 to fine-tuning can improve merging performance. However, these approaches adjust the fine-
 499 tuning procedure itself, for example by updating only selected submodules (Jin et al., 2025) or pa-
 500 rameters (Iurada et al., 2025), using sharpness-aware optimization (Lee et al., 2025), or employing
 501 linearization-based updates (Tang et al., 2024b; Ortiz-Jimenez et al., 2023). In contrast, our work
 502 analyzes how *standard* fine-tuning protocols, without merging-specific adjustments, affect down-
 503 stream merging and MoErging performance, providing a complementary perspective on merging
 504 behavior under the most commonly used training procedures.

505 **Expert training time** Most model merging and MoErging papers do not examine how expert
 506 fine-tuning affects downstream upcycling, with two notable exceptions. Zhou et al. (2025) show
 507 that the effectiveness of task-vector based approaches is largely driven by first-epoch gradients and
 508 propose alternating 1-epoch fine-tuning and merging. While they note that less training can improve
 509 accuracy, they only test 1, which can yield either overtrained or undertrained experts depending
 510 on dataset size. Pari et al. (2024) observe representational incompatibilities when merging highly
 511 specialized experts, but study only two-model merges and propose bypassing merging altogether by
 512 using MoErging. To our knowledge, we are the first to systematically link expert training duration
 513 to downstream upcycling outcomes, analyze merging through example difficulty, and propose an
 514 early-stopping strategy that adapts to dataset heterogeneity. Finally, although TIES Merging (Yadav
 515 et al., 2023) uses early stopping, it is only used to avoid expert overfitting and its effect on merging
 516 is not studied.

517 **Overtraining in pre-training** Analogous to our work, others have studied how scaling pre-
 518 training impacts downstream fine-tuning. In a large-scale vision study, Abnar et al. (2022) found that
 519 as pre-training accuracy improves, fine-tuning saturates. Recently, Springer et al. (2025) show that
 520 over-training LLMs during pre-training can harm fine-tuned in- and out-of-distribution performance.

7 CONCLUSION

523 In this paper, we challenged the assumption that better fine-tuned experts yield better upcycling per-
 524 formance. Across multiple merging methods, model families and sizes, and for both fully fine-tuned
 525 and LoRA-adapted models, we found that optimal merging occurs well before full convergence,
 526 often when experts are less accurate on their original tasks. For MoErging, continued fine-tuning
 527 of LoRA experts even degrades downstream multi-task performance. We attribute this to a shift
 528 in training dynamics: as fine-tuning progresses, training becomes dominated by memorization of
 529 difficult examples, leading to idiosyncratic parameter updates and negative parameter interference.
 530 Finally, we show that simple early stopping strategies mitigate overtraining and can even yield su-
 531 perior upcycling performance.

532 Our findings have important implications for the sharing of model versions and adapters and the
 533 evaluation of upcycling pipelines. **Publish intermediate checkpoints:** Releasing not only final but
 534 also intermediate checkpoints is crucial, as the best upcycling point may precede convergence. In
 535 practice, even a single intermediate checkpoint, extracted when validation accuracy starts to plateau,
 536 is likely sufficient for achieving close-to-optimal upcycling performance, as supported by our early
 537 stopping experiments. **Prioritize early-stopped experts:** When training experts in-house, aggres-
 538 sive early stopping can outperform convergence for downstream upcycling. Since upcycling reuses
 539 checkpoints and amortizes sunk costs, our findings can help reduce the future computational and
 environmental footprint of training AI models.

540 **8 REPRODUCIBILITY STATEMENT**
 541

542 We have taken several steps to ensure the reproducibility of our work. In Section 2.5 we describe
 543 the exact models, datasets, and codebases used, as well as the machine learning frameworks and
 544 hardware employed. All frameworks and codebases are open-sourced and publicly available, and our
 545 exact codebase is provided as supplementary material. In addition, our main text and the Appendix
 546 include all relevant details and a description of our hyperparameter tuning procedures, ensuring that
 547 our experiments can be fully reproduced.

548
 549 **REFERENCES**
 550

551 Samira Abnar, Mostafa Dehghani, Behnam Neyshabur, and Hanie Sedghi. Exploring the limits of
 552 large scale pre-training. In *International Conference on Learning Representations*, 2022. URL
 553 <https://openreview.net/forum?id=V3C8p78sDa>.

554 Idan Attias, Gintare Karolina Dziugaite, Mahdi Haghifam, Roi Livni, and Daniel M Roy. Information
 555 complexity of stochastic convex optimization: Applications to generalization and memorization.
 556 *arXiv preprint arXiv:2402.09327*, 2024.

557 Edward Beeching, Clémentine Fourrier, Nathan Habib, Sheon Han, Nathan Lambert, Nazneen Ra-
 558 jani, Omar Sanseviero, Lewis Tunstall, and Thomas Wolf. Open LLM Leaderboard (2023–2024).
 559 https://huggingface.co/spaces/open-llm-leaderboard-old/open_llm_leaderboard, 2023. Accessed: 2025-04-29.

560 Gong Cheng, Junwei Han, and Xiaoqiang Lu. Remote sensing image scene classification: Bench-
 561 mark and state of the art. *Proceedings of the IEEE*, 105(10):1865–1883, Oct 2017. ISSN 1558-
 562 2256. doi: 10.1109/jproc.2017.2675998. URL <http://dx.doi.org/10.1109/JPROC.2017.2675998>.

563 Leshem Choshen, Elad Venezian, Noam Slonim, and Yoav Katz. Fusing finetuned models for better
 564 pretraining, 2022. URL <https://arxiv.org/abs/2204.03044>.

565 Mircea Cimpoi, Subhransu Maji, Iasonas Kokkinos, Sammy Mohamed, and Andrea Vedaldi. De-
 566 scribing textures in the wild. In *Proceedings of the IEEE Conference on Computer Vision and
 567 Pattern Recognition (CVPR)*, June 2014.

568 MohammadReza Davari and Eugene Belilovsky. Model breadcrumbs: Scaling multi-task model
 569 merging with sparse masks. In *Computer Vision – ECCV 2024: 18th European Conference,
 570 Milan, Italy, September 29–October 4, 2024, Proceedings, Part LXXV*, pp. 270–287, Berlin, Hei-
 571 delberg, 2024. Springer-Verlag. ISBN 978-3-031-73225-6. doi: 10.1007/978-3-031-73226-3_16.
 572 URL https://doi.org/10.1007/978-3-031-73226-3_16.

573 Pala Tej Deep, Rishabh Bhardwaj, and Soujanya Poria. Della-merging: Reducing interference in
 574 model merging through magnitude-based sampling, 2024. URL <https://arxiv.org/abs/2406.11617>.

575 DeepSeek-AI. Deepseek-v3 technical report, 2024. URL <https://arxiv.org/abs/2412.19437>.

576 Li Deng. The mnist database of handwritten digit images for machine learning research. *IEEE
 577 Signal Processing Magazine*, 29(6):141–142, 2012.

578 Jacob Devlin, Ming-Wei Chang, Kenton Lee, and Kristina Toutanova. Bert: Pre-training of deep
 579 bidirectional transformers for language understanding, 2019. URL <https://arxiv.org/abs/1810.04805>.

580 Alexey Dosovitskiy, Lucas Beyer, Alexander Kolesnikov, Dirk Weissenborn, Xiaohua Zhai, Thomas
 581 Unterthiner, Mostafa Dehghani, Matthias Minderer, Georg Heigold, Sylvain Gelly, Jakob Uszko-
 582 reit, and Neil Houlsby. An image is worth 16x16 words: Transformers for image recogni-
 583 tion at scale. In *International Conference on Learning Representations*, 2021. URL <https://openreview.net/forum?id=YicbFdNTTy>.

594 Vitaly Feldman. Does learning require memorization? a short tale about a long tail. In *Proceedings*
 595 *of the 52nd Annual ACM SIGACT Symposium on Theory of Computing*, pp. 954–959, 2020.
 596

597 Vitaly Feldman and Chiyuan Zhang. What neural networks memorize and why: Discovering the
 598 long tail via influence estimation. In H. Larochelle, M. Ranzato, R. Hadsell, M.F. Balcan, and
 599 H. Lin (eds.), *Advances in Neural Information Processing Systems*, volume 33, pp. 2881–2891.
 600 Curran Associates, Inc., 2020. URL https://proceedings.neurips.cc/paper_files/paper/2020/file/1e14bfe2714193e7af5abc64ecbd6b46-Paper.pdf.
 601

602 Jonathan Frankle, Gintare Karolina Dziugaite, Daniel Roy, and Michael Carbin. Linear mode
 603 connectivity and the lottery ticket hypothesis. In Hal Daumé III and Aarti Singh (eds.), *Pro-
 604 ceedings of the 37th International Conference on Machine Learning*, volume 119 of *Proceed-
 605 ings of Machine Learning Research*, pp. 3259–3269. PMLR, 13–18 Jul 2020. URL <https://proceedings.mlr.press/v119/frankle20a.html>.
 606

607 Charles Goddard, Shamane Siriwardhana, Malikeh Ehghaghi, Luke Meyers, Vladimir Karpukhin,
 608 Brian Benedict, Mark McQuade, and Jacob Solawetz. Arcee’s MergeKit: A toolkit for merg-
 609 ing large language models. In Franck Dernoncourt, Daniel Preoṭiuc-Pietro, and Anastasia
 610 Shimorina (eds.), *Proceedings of the 2024 Conference on Empirical Methods in Natural Lan-
 611 guage Processing: Industry Track*, pp. 477–485, Miami, Florida, US, November 2024. Associa-
 612 tion for Computational Linguistics. doi: 10.18653/v1/2024.emnlp-industry.36. URL <https://aclanthology.org/2024.emnlp-industry.36>.
 613

614

615 Aaron Grattafiori et al. The llama 3 herd of models, 2024. URL <https://arxiv.org/abs/2407.21783>.
 616

617 Ethan He, Abhinav Khattar, Ryan Prenger, Vijay Korthikanti, Zijie Yan, Tong Liu, Shiqing Fan,
 618 Ashwath Aithal, Mohammad Shoeybi, and Bryan Catanzaro. Upcycling large language models
 619 into mixture of experts, 2024. URL <https://arxiv.org/abs/2410.07524>.
 620

621 Patrick Helber, Benjamin Bischke, Andreas Dengel, and Damian Borth. Eurosat: A novel dataset
 622 and deep learning benchmark for land use and land cover classification. *IEEE Journal of Selected
 623 Topics in Applied Earth Observations and Remote Sensing*, 2019.
 624

625 Edward J Hu, yelong shen, Phillip Wallis, Zeyuan Allen-Zhu, Yuanzhi Li, Shean Wang, Lu Wang,
 626 and Weizhu Chen. LoRA: Low-rank adaptation of large language models. In *International Con-
 627 ference on Learning Representations*, 2022. URL <https://openreview.net/forum?id=nZeVKeFYf9>.
 628

629 Chengsong Huang, Qian Liu, Bill Yuchen Lin, Tianyu Pang, Chao Du, and Min Lin. Lorahub: Effi-
 630 cient cross-task generalization via dynamic LoRA composition. In *First Conference on Language
 631 Modeling*, 2024. URL <https://openreview.net/forum?id=TrloAXEJ2B>.
 632

633 Gabriel Ilharco, Mitchell Wortsman, Ross Wightman, Cade Gordon, Nicholas Carlini, Rohan Taori,
 634 Achal Dave, Vaishaal Shankar, Hongseok Namkoong, John Miller, Hannaneh Hajishirzi, Ali
 635 Farhadi, and Ludwig Schmidt. Openclip, July 2021. URL <https://doi.org/10.5281/zenodo.5143773>. If you use this software, please cite it as below.
 636

637 Gabriel Ilharco, Marco Túlio Ribeiro, Mitchell Wortsman, Ludwig Schmidt, Hannaneh Hajishirzi,
 638 and Ali Farhadi. Editing models with task arithmetic. In *The Eleventh International Confer-
 639 ence on Learning Representations*, 2023. URL <https://openreview.net/forum?id=6t0Kwf8-jrj>.
 640

642 Leonardo Iurada, Marco Ciccone, and Tatiana Tommasi. Efficient model editing with task-localized
 643 sparse fine-tuning. In *The Thirteenth International Conference on Learning Representations*,
 644 2025. URL <https://openreview.net/forum?id=TDyE2iuvyc>.
 645

646 Pavel Izmailov, Dmitrii Podoprikhin, Timur Garipov, Dmitry Vetrov, and Andrew G. Wilson. Aver-
 647 aging weights leads to wider optima and better generalization. In Amir Globerson and Ricardo
 648 Silva (eds.), *Uncertainty in Artificial Intelligence*. AUAI Press, 2018.

648 Ruochen Jin, Bojian Hou, Jiancong Xiao, Weijie J Su, and Li Shen. Fine-tuning attention modules
 649 only: Enhancing weight disentanglement in task arithmetic. In *The Thirteenth International Con-*
 650 *ference on Learning Representations*, 2025. URL [https://openreview.net/forum?](https://openreview.net/forum?id=dj0TkJcVI)
 651 [id=dj0TkJcVI](https://openreview.net/forum?id=dj0TkJcVI).

652 Xisen Jin, Xiang Ren, Daniel Preotiuc-Pietro, and Pengxiang Cheng. Dataless knowledge fusion
 653 by merging weights of language models. In *The Eleventh International Conference on Learning*
 654 *Representations*, 2023. URL <https://openreview.net/forum?id=FCnohuR6AnM>.

655 Nikhil Kandpal, Brian Lester, Mohammed Muqeeth, Anisha Mascarenhas, Monty Evans, Vishal
 656 Baskaran, Tenghao Huang, Haokun Liu, and Colin Raffel. Git-theta: A git extension for collabora-
 657 tive development of machine learning models. In Andreas Krause, Emma Brunskill, Kyunghyun
 658 Cho, Barbara Engelhardt, Sivan Sabato, and Jonathan Scarlett (eds.), *Proceedings of the 40th In-*
 659 *ternational Conference on Machine Learning*, volume 202 of *Proceedings of Machine Learning*
 660 *Research*, pp. 15708–15719. PMLR, 23–29 Jul 2023. URL <https://proceedings.mlr.press/v202/kandpal23b.html>.

661 Tushar Khot, Peter Clark, Michal Guerquin, Peter Jansen, and Ashish Sabharwal. Qasc: A dataset
 662 for question answering via sentence composition. *Proceedings of the AAAI Conference on*
 663 *Artificial Intelligence*, 34(05):8082–8090, Apr. 2020. doi: 10.1609/aaai.v34i05.6319. URL
 664 <https://ojs.aaai.org/index.php/AAAI/article/view/6319>.

665 Jonathan Krause, Michael Stark, Jia Deng, and Li Fei-Fei. 3d object representations for fine-grained
 666 categorization. In *Proceedings of the IEEE International Conference on Computer Vision (ICCV)*
 667 *Workshops*, June 2013.

668 Devin Kwok, Nikhil Anand, Jonathan Frankle, Gintare Karolina Dziugaite, and David Rolnick.
 669 Dataset difficulty and the role of inductive bias. *arXiv preprint arXiv:2401.01867*, 2024.

670 Yeoreum Lee, Jinwook Jung, and Sungyong Baik. Mitigating parameter interference in model merg-
 671 ing via sharpness-aware fine-tuning. In *The Thirteenth International Conference on Learning*
 672 *Representations*, 2025. URL <https://openreview.net/forum?id=eaTqsptDPL>.

673 Hector J. Levesque, Ernest Davis, and Leora Morgenstern. The winograd schema challenge. In *Pro-*
 674 *ceedings of the Thirteenth International Conference on Principles of Knowledge Representation*
 675 *and Reasoning*, KR’12, pp. 552–561. AAAI Press, 2012. ISBN 9781577355601.

676 Haokun Liu, Derek Tam, Muqeeth Mohammed, Jay Mohta, Tenghao Huang, Mohit Bansal, and
 677 Colin Raffel. Few-shot parameter-efficient fine-tuning is better and cheaper than in-context learn-
 678 ing. In Alice H. Oh, Alekh Agarwal, Danielle Belgrave, and Kyunghyun Cho (eds.), *Advances in*
 679 *Neural Information Processing Systems*, 2022. URL [https://openreview.net/forum?](https://openreview.net/forum?id=rBCvMG-JsPd)
 680 [id=rBCvMG-JsPd](https://openreview.net/forum?id=rBCvMG-JsPd).

681 Ilya Loshchilov and Frank Hutter. Decoupled weight decay regularization. In *International Confer-*
 682 *ence on Learning Representations*, 2019. URL <https://openreview.net/forum?id=Bkg6RiCqY7>.

683 Michael S Matena and Colin A Raffel. Merging models with fisher-weighted averaging. In S. Koyejo, S. Mohamed, A. Agarwal, D. Belgrave, K. Cho, and A. Oh (eds.), *Advances in*
 684 *Neural Information Processing Systems*, volume 35, pp. 17703–17716. Curran Associates, Inc.,
 685 2022. URL https://proceedings.neurips.cc/paper_files/paper/2022/file/70c26937fbf3d4600b69a129031b66ec-Paper-Conference.pdf.

686 Brendan McMahan, Eider Moore, Daniel Ramage, Seth Hampson, and Blaise Aguera y Ar-
 687 cas. Communication-Efficient Learning of Deep Networks from Decentralized Data. In Aarti Singh and Jerry Zhu (eds.), *Proceedings of the 20th International Conference on Artifi-*
 688 *cial Intelligence and Statistics*, volume 54 of *Proceedings of Machine Learning Research*, pp.
 689 1273–1282. PMLR, 20–22 Apr 2017. URL <https://proceedings.mlr.press/v54/mcmahan17a.html>.

690 Mohammed Muqeeth, Haokun Liu, Yufan Liu, and Colin Raffel. Learning to route among special-
 691 ized experts for zero-shot generalization, 2024. URL <https://arxiv.org/abs/2402.05859>.

702 Yuval Netzer, Tao Wang, Adam Coates, Alessandro Bissacco, Bo Wu, and Andrew Y. Ng. Reading
 703 digits in natural images with unsupervised feature learning. *NIPS Workshop on Deep Learning*
 704 and *Unsupervised Feature Learning*, 2011.

705 Behnam Neyshabur, Hanie Sedghi, and Chiyuan Zhang. What is being transferred in trans-
 706 fer learning? In H. Larochelle, M. Ranzato, R. Hadsell, M.F. Balcan, and H. Lin (eds.), *Advances in Neural Infor-
 707 mation Processing Systems*, volume 33, pp. 512–523. Curran Associates, Inc., 2020. URL <https://proceedings.neurips.cc/paper/2020/file/0607f4c705595b911a4f3e7a127b44e0-Paper.pdf>.

708 Guillermo Ortiz-Jimenez, Alessandro Favero, and Pascal Frossard. Task arithmetic in
 709 the tangent space: Improved editing of pre-trained models. In A. Oh, T. Naumann,
 710 A. Globerson, K. Saenko, M. Hardt, and S. Levine (eds.), *Advances in Neural Infor-
 711 mation Processing Systems*, volume 36, pp. 66727–66754. Curran Associates, Inc.,
 712 2023. URL https://proceedings.neurips.cc/paper_files/paper/2023/file/d28077e5ff52034cd35b4aa15320caeae-Paper-Conference.pdf.

713 Oleksiy Ostapenko, Zhan Su, Edoardo Ponti, Laurent Charlin, Nicolas Le Roux, Lucas Caccia, and
 714 Alessandro Sordoni. Towards modular LLMs by building and reusing a library of LoRAs. In
 715 Ruslan Salakhutdinov, Zico Kolter, Katherine Heller, Adrian Weller, Nuria Oliver, Jonathan Scar-
 716 lett, and Felix Berkenkamp (eds.), *Proceedings of the 41st International Conference on Machine
 717 Learning*, volume 235 of *Proceedings of Machine Learning Research*, pp. 38885–38904. PMLR,
 718 21–27 Jul 2024. URL <https://proceedings.mlr.press/v235/ostapenko24a.html>.

719 Jyothish Pari, Samy Jelassi, and Pulkit Agrawal. Collective model intelligence requires compatible
 720 specialization, 2024. URL <https://arxiv.org/abs/2411.02207>.

721 Adam Paszke, Sam Gross, Francisco Massa, Adam Lerer, James Bradbury, Gregory Chanan, Trevor
 722 Killeen, Zeming Lin, Natalia Gimelshein, Luca Antiga, Alban Desmaison, Andreas Kopf, Edward
 723 Yang, Zachary DeVito, Martin Raison, Alykhan Tejani, Sasank Chilamkurthy, Benoit Steiner,
 724 Lu Fang, Junjie Bai, and Soumith Chintala. Pytorch: An imperative style, high-performance
 725 deep learning library. In H. Wallach, H. Larochelle, A. Beygelzimer, F. d’Alché-Buc, E. Fox,
 726 and R. Garnett (eds.), *Advances in Neural Information Processing Systems*, volume 32. Cur-
 727 ran Associates, Inc., 2019. URL https://proceedings.neurips.cc/paper_files/paper/2019/file/bdbca288fee7f92f2bfa9f7012727740-Paper.pdf.

728 Mansheej Paul, Surya Ganguli, and Gintare Karolina Dziugaite. Deep learning on a
 729 data diet: Finding important examples early in training. In M. Ranzato, A. Beygelz-
 730 imer, Y. Dauphin, P.S. Liang, and J. Wortman Vaughan (eds.), *Advances in Neural Infor-
 731 mation Processing Systems*, volume 34, pp. 20596–20607. Curran Associates, Inc.,
 732 2021. URL https://proceedings.neurips.cc/paper_files/paper/2021/file/ac56f8fe9ee3e4a365f29f0f1957c55-Paper.pdf.

733 Jonas Pfeiffer, Andreas Rücklé, Clifton Poth, Aishwarya Kamath, Ivan Vulić, Sebastian Ruder,
 734 Kyunghyun Cho, and Iryna Gurevych. AdapterHub: A framework for adapting transformers.
 735 In Qun Liu and David Schlangen (eds.), *Proceedings of the 2020 Conference on Empirical
 736 Methods in Natural Language Processing: System Demonstrations*, pp. 46–54, Online, October
 737 2020. Association for Computational Linguistics. doi: 10.18653/v1/2020.emnlp-demos.7. URL
 738 <https://aclanthology.org/2020.emnlp-demos.7/>.

739 Alec Radford, Jong Wook Kim, Chris Hallacy, Aditya Ramesh, Gabriel Goh, Sandhini Agar-
 740 wal, Girish Sastry, Amanda Askell, Pamela Mishkin, Jack Clark, Gretchen Krueger, and Ilya
 741 Sutskever. Learning transferable visual models from natural language supervision. In Marina
 742 Meila and Tong Zhang (eds.), *Proceedings of the 38th International Conference on Machine
 743 Learning*, volume 139 of *Proceedings of Machine Learning Research*, pp. 8748–8763. PMLR,
 744 18–24 Jul 2021. URL <https://proceedings.mlr.press/v139/radford21a.html>.

745 Colin Raffel, Noam Shazeer, Adam Roberts, Katherine Lee, Sharan Narang, Michael Matena, Yanqi
 746 Zhou, Wei Li, and Peter J. Liu. Exploring the limits of transfer learning with a unified text-to-
 747 text transformer. *Journal of Machine Learning Research*, 21(140):1–67, 2020. URL <http://jmlr.org/papers/v21/20-074.html>.

756 Keisuke Sakaguchi, Ronan Le Bras, Chandra Bhagavatula, and Yejin Choi. Winogrande: An ad-
 757 versarial winograd schema challenge at scale. *Proceedings of the AAAI Conference on Artifi-*
 758 *cial Intelligence*, 34(05):8732–8740, Apr. 2020. doi: 10.1609/aaai.v34i05.6399. URL <https://ojs.aaai.org/index.php/AAAI/article/view/6399>.

760 Ekansh Sharma, Daniel M Roy, and Gintare Karolina Dziugaite. The non-local model merging
 761 problem: Permutation symmetries and variance collapse. *arXiv preprint arXiv:2410.12766*, 2024.

763 Rishi Sharma, James Allen, Omid Bakhshandeh, and Nasrin Mostafazadeh. Tackling the story end-
 764 ing biases in the story cloze test. In Iryna Gurevych and Yusuke Miyao (eds.), *Proceedings of the*
 765 *56th Annual Meeting of the Association for Computational Linguistics (Volume 2: Short Papers)*,
 766 pp. 752–757, Melbourne, Australia, July 2018. Association for Computational Linguistics. doi:
 767 10.18653/v1/P18-2119. URL <https://aclanthology.org/P18-2119/>.

768 Noam Shazeer, *Azalia Mirhoseini, *Krzysztof Maziarz, Andy Davis, Quoc Le, Geoffrey Hin-
 769 ton, and Jeff Dean. Outrageously large neural networks: The sparsely-gated mixture-of-
 770 experts layer. In *International Conference on Learning Representations*, 2017. URL <https://openreview.net/forum?id=B1ckMDqlg>.

772 Ben Sorscher, Robert Geirhos, Shashank Shekhar, Surya Ganguli, and Ari Morcos. Be-
 773 yond neural scaling laws: beating power law scaling via data pruning. In S. Koyejo,
 774 S. Mohamed, A. Agarwal, D. Belgrave, K. Cho, and A. Oh (eds.), *Advances in Neu-*
 775 *ral Information Processing Systems*, volume 35, pp. 19523–19536. Curran Associates, Inc.,
 776 2022. URL https://proceedings.neurips.cc/paper_files/paper/2022/file/7b75da9b61eda40fa35453ee5d077df6-Paper-Conference.pdf.

778 779 Jacob Mitchell Springer, Sachin Goyal, Kaiyue Wen, Tanishq Kumar, Xiang Yue, Sadhika Malladi,
 780 Graham Neubig, and Aditi Raghunathan. Overtrained language models are harder to fine-tune,
 781 2025. URL <https://arxiv.org/abs/2503.19206>.

782 783 J. Stallkamp, M. Schlipsing, J. Salmen, and C. Igel. Man vs. computer: Benchmarking machine
 784 learning algorithms for traffic sign recognition. *Neural Networks*, 32(0):–, 2012. ISSN 0893-6080.
 785 doi: 10.1016/j.neunet.2012.02.016. URL <http://www.sciencedirect.com/science/article/pii/S0893608012000457>.

786 787 Stanford-CRFM. On the opportunities and risks of foundation models. *ArXiv*, 2021. URL <https://crfm.stanford.edu/assets/report.pdf>.

788 789 George Stoica, Pratik Ramesh, Boglarka Ecsedi, Leshem Choshen, and Judy Hoffman. Model
 790 merging with SVD to tie the knots. In *The Thirteenth International Conference on Learning*
 791 *Representations*, 2025. URL <https://openreview.net/forum?id=67X93aZHII>.

792 793 Oyvind Tafjord, Matt Gardner, Kevin Lin, and Peter Clark. QuaRTz: An open-domain dataset
 794 of qualitative relationship questions. In Kentaro Inui, Jing Jiang, Vincent Ng, and Xiao-
 795 jun Wan (eds.), *Proceedings of the 2019 Conference on Empirical Methods in Natural Lan-*
 796 *guage Processing and the 9th International Joint Conference on Natural Language Processing*
 797 (*EMNLP-IJCNLP*), pp. 5941–5946, Hong Kong, China, November 2019. Association for Com-
 798 putational Linguistics. doi: 10.18653/v1/D19-1608. URL <https://aclanthology.org/D19-1608/>.

799 800 Derek Tam, Mohit Bansal, and Colin Raffel. Merging by matching models in task parame-
 801 ter subspaces. *Transactions on Machine Learning Research*, 2024. ISSN 2835-8856. URL
 802 <https://openreview.net/forum?id=qNGo6ghWFB>.

803 804 Anke Tang, Li Shen, Yong Luo, Yibing Zhan, Han Hu, Bo Du, Yixin Chen, and Dacheng Tao.
 805 Parameter-efficient multi-task model fusion with partial linearization. In *The Twelfth Interna-*
 806 *tional Conference on Learning Representations*, 2024a. URL <https://openreview.net/forum?id=iynRvVVAmH>.

807 808 Anke Tang, Li Shen, Yong Luo, Yibing Zhan, Han Hu, Bo Du, Yixin Chen, and Dacheng Tao.
 809 Parameter-efficient multi-task model fusion with partial linearization. In *The Twelfth Interna-*
 810 *tional Conference on Learning Representations*, 2024b. URL <https://openreview.net/forum?id=iynRvVVAmH>.

810 Gemma Team. Gemma 3 technical report, 2025. URL <https://arxiv.org/abs/2503.19786>.

811

812

813 Mariya Toneva, Alessandro Sordoni, Remi Tachet des Combes, Adam Trischler, Yoshua Bengio,
814 and Geoffrey J. Gordon. An empirical study of example forgetting during deep neural network
815 learning. In *International Conference on Learning Representations*, 2019. URL <https://openreview.net/forum?id=BJlxm30cKm>.

816

817 Thomas Wolf, Lysandre Debut, Victor Sanh, Julien Chaumond, Clement Delangue, Anthony Moi,
818 Pierrick Cistac, Tim Rault, Rémi Louf, Morgan Funtowicz, and Jamie Brew. Huggingface’s
819 transformers: State-of-the-art natural language processing. *CoRR*, abs/1910.03771, 2019. URL
820 <http://arxiv.org/abs/1910.03771>.

821

822 Mitchell Wortsman, Gabriel Ilharco, Jong Wook Kim, Mike Li, Simon Kornblith, Rebecca Roelofs,
823 Raphael Gontijo Lopes, Hannaneh Hajishirzi, Ali Farhadi, Hongseok Namkoong, and Ludwig
824 Schmidt. Robust fine-tuning of zero-shot models. In *Proceedings of the IEEE/CVF Conference
825 on Computer Vision and Pattern Recognition (CVPR)*, pp. 7959–7971, June 2022.

826

827 J. Xiao, J. Hays, K. A. Ehinger, A. Oliva, and A. Torralba. Sun database: Large-scale scene recog-
828 nition from abbey to zoo. In *2010 IEEE Computer Society Conference on Computer Vision and
829 Pattern Recognition*, pp. 3485–3492, June 2010. doi: 10.1109/CVPR.2010.5539970.

830

831 Prateek Yadav, Derek Tam, Leshem Choshen, Colin Raffel, and Mohit Bansal. TIES-merging: Re-
832 solving interference when merging models. In *Thirty-seventh Conference on Neural Information
833 Processing Systems*, 2023. URL <https://openreview.net/forum?id=xtaX3WyCj1>.

834

835 Prateek Yadav, Colin Raffel, Mohammed Muqeeth, Lucas Caccia, Haokun Liu, Tianlong Chen,
836 Mohit Bansal, Leshem Choshen, and Alessandro Sordoni. A survey on model moerging: Re-
837 cycling and routing among specialized experts for collaborative learning, 2024. URL <https://arxiv.org/abs/2408.07057>.

838

839 Enneng Yang, Li Shen, Guibing Guo, Xingwei Wang, Xiaochun Cao, Jie Zhang, and Dacheng Tao.
840 Model merging in llms, mllms, and beyond: Methods, theories, applications and opportunities.
841 *arXiv preprint arXiv:2408.07666*, 2024.

842

843 Yi Yang, Wen-tau Yih, and Christopher Meek. WikiQA: A challenge dataset for open-domain
844 question answering. In Lluís Márquez, Chris Callison-Burch, and Jian Su (eds.), *Proceedings
845 of the 2015 Conference on Empirical Methods in Natural Language Processing*, pp. 2013–2018,
846 Lisbon, Portugal, September 2015. Association for Computational Linguistics. doi: 10.18653/v1/
847 D15-1237. URL <https://aclanthology.org/D15-1237/>.

848

849 Le Yu, Bowen Yu, Haiyang Yu, Fei Huang, and Yongbin Li. Language models are super mario:
850 Absorbing abilities from homologous models as a free lunch. In Ruslan Salakhutdinov, Zico
851 Kolter, Katherine Heller, Adrian Weller, Nuria Oliver, Jonathan Scarlett, and Felix Berkenkamp
852 (eds.), *Proceedings of the 41st International Conference on Machine Learning*, volume 235 of
853 *Proceedings of Machine Learning Research*, pp. 57755–57775. PMLR, 21–27 Jul 2024. URL
854 <https://proceedings.mlr.press/v235/yu24p.html>.

855

856 Qizhen Zhang, Nikolas Gritsch, Dwaraknath Gnaneshwar, Simon Guo, David Cairuz, Bharat
857 Venkitesh, Jakob Nicolaus Foerster, Phil Blunsom, Sebastian Ruder, Ahmet Üstün, and Acyr
858 Locatelli. BAM! just like that: Simple and efficient parameter upcycling for mixture of experts.
859 In *The Thirty-eighth Annual Conference on Neural Information Processing Systems*, 2024. URL
860 <https://openreview.net/forum?id=BDrlWQTrfyI>.

861

862 Yuan Zhang, Jason Baldridge, and Luheng He. PAWS: Paraphrase adversaries from word scram-
863 bling. In Jill Burstein, Christy Doran, and Thamar Solorio (eds.), *Proceedings of the 2019 Con-
864 ference of the North American Chapter of the Association for Computational Linguistics: Human
865 Language Technologies, Volume 1 (Long and Short Papers)*, pp. 1298–1308, Minneapolis, Min-
866 nesota, June 2019. Association for Computational Linguistics. doi: 10.18653/v1/N19-1131. URL
867 <https://aclanthology.org/N19-1131/>.

868

869 Luca Zhou, Daniele Solombrino, Donato Crisostomi, Maria Sofia Bucarelli, Fabrizio Silvestri, and
870 Emanuele Rodolà. Atm: Improving model merging by alternating tuning and merging, 2025.
871 URL <https://arxiv.org/abs/2411.03055>.

864 **A ADDITIONAL RELATED WORK**
865

866 The simplest approach, parameter averaging, was shown to lead to better generalization when used
 867 on checkpoints from the same training trajectory (Izmailov et al., 2018) and was popularized in
 868 federated learning with FedAvg (McMahan et al., 2017). Recently, parameter averaging was also
 869 shown to be useful in the context of robust fine-tuning (Wortsman et al., 2022) and to obtain better
 870 pre-trained models (Choshen et al., 2022). When merging multiple fine-tuned versions of the same
 871 pre-trained model, Fisher-weighted averaging (Matena & Raffel, 2022) and related methods improve
 872 upon this simple averaging by adjusting per-parameter contributions (Jin et al., 2023; Tam et al.,
 873 2024). Task arithmetic based methods rely on the computation of task vectors, which are then
 874 summed, scaled and added back to the pretrained model (Ilharco et al., 2023) to give it multi-task
 875 capabilities. Pruning the task vector parameters (Yadav et al., 2023; Davari & Belilovsky, 2024;
 876 Yu et al., 2024; Deep et al., 2024) and selectively combining them to reduce negative interference
 877 (Yadav et al., 2023) further benefits performance.

878 Sharma et al. (2024) explores merging of experts that were trained from different or poorly performing
 879 pre-trained models.

880
881 **B TUNING MERGING HYPERPARAMETERS**
882

883 Several merging methods require careful hyperparameter tuning to achieve optimal performance. In
 884 particular, Task Arithmetic, TIES, and DARE each apply a scaling factor α to their task-vector sums
 885 before adding them to the pretrained weights; TIES and DARE additionally specify a percentage
 886 k of weights to retain after pruning. As is standard, we select the best α , k values by maximizing
 887 merging accuracy on a held-out validation set. All merging accuracies reported in the main text are
 888 evaluated on the test set using hyperparameters selected via validation performance. We followed
 889 the hyperparameter configurations from the original papers (Ilharco et al., 2023; Yadav et al., 2023;
 890 Yu et al., 2024), adjusting them as needed to optimize performance in our experimental settings.

891 **Crucially, we perform tuning of merging hyperparameters for each individual merging exper-
 892 iment, i.e. the tuning is done for each different number of training steps and each different
 893 random seed across all our settings.**

894 **Vision setting:** Following (Ilharco et al., 2023), we reserve 10% of the training data for validation
 895 and train the ViT models on the remaining 90%. We tune the following hyperparameter values using
 896 the validation set:

897
898 • **Task Arithmetic:** $\alpha \in \{0.05, 0.1, \dots, 1\}$
 899 • **TIES:** $\alpha \in \{0.5, 0.6, \dots, 1.5\}$ and $k \in \{10, 20, 30\}$
 900 • **DARE:** $\alpha \in \{0.05, 0.1, \dots, 0.55\}$ and $k \in \{10, 20, 30\}$

902 **NLP setting:** We adopt the validation splits from (Yadav et al., 2023) and evaluate the following
 903 hyperparameter values:
 904

905 • **Task Arithmetic:** $\alpha \in \{0.1, 0.2, \dots, 1\}$
 906 • **TIES:** $\alpha \in \{0.8, 0.9, \dots, 2.1\}$ and $k \in \{10, 20, 30\}$

908 **C USING THE RAW, UN-NORMALIZED ACCURACY**
909

910 The *normalized accuracy* is a very common metric used to compare model merging methods (Ilharco
 911 et al., 2023; Yadav et al., 2023). However, because the normalized accuracy depends on both the
 912 merged model’s performance and that of the experts, it isn’t suitable for settings like ours where
 913 different sets of experts are used and compared.

914 The core issue is that normalized accuracy, defined as (merged_accuracy / expert_accuracy), is a
 915 relative metric designed to compare different merging methods when the set of experts (the denom-
 916 inator) is fixed. Papers that propose a novel model merging method are justified in using this metric
 917 by the fact that they have a fixed set of experts and they are comparing merging methods, therefore

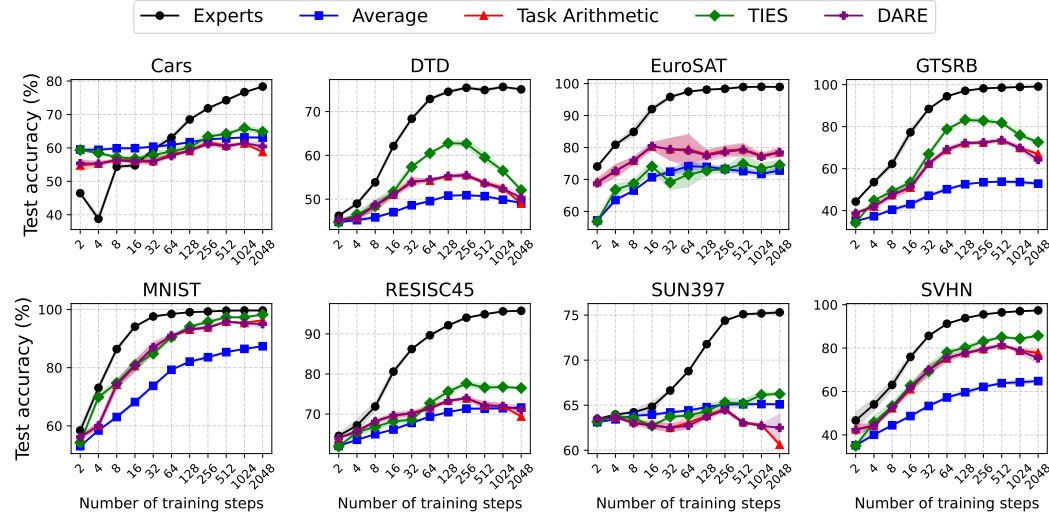
918 only the numerator changes. In our study, the experts themselves are the primary variable, as their
919 training duration and performance change in each experiment, therefore the denominator changes
920 from one merging experiment to another. This creates paradoxical situations that make the metric
921 misleading for our purposes. For example consider the following scenario:
922

- 923 • **Case 1 (Undertraining):** Experts trained for only a few steps have very low absolute
924 accuracy (e.g., 60%). When merged, they interfere very little since they’re all relatively
925 close in parameter space to the zeroshot model, so the merged model also achieves around
926 60% accuracy. This yields a normalized accuracy near 100%, despite the models being bad
927 at solving the considered tasks.
- 928 • **Case 2 (Optimal Training):** Experts trained for longer have high accuracy (e.g., 90%).
929 Merging them results in a high-performing model with 85% absolute accuracy. However,
930 the normalized accuracy is only $85/90 = 94.4\%$ due to negative interference caused by
931 longer training.

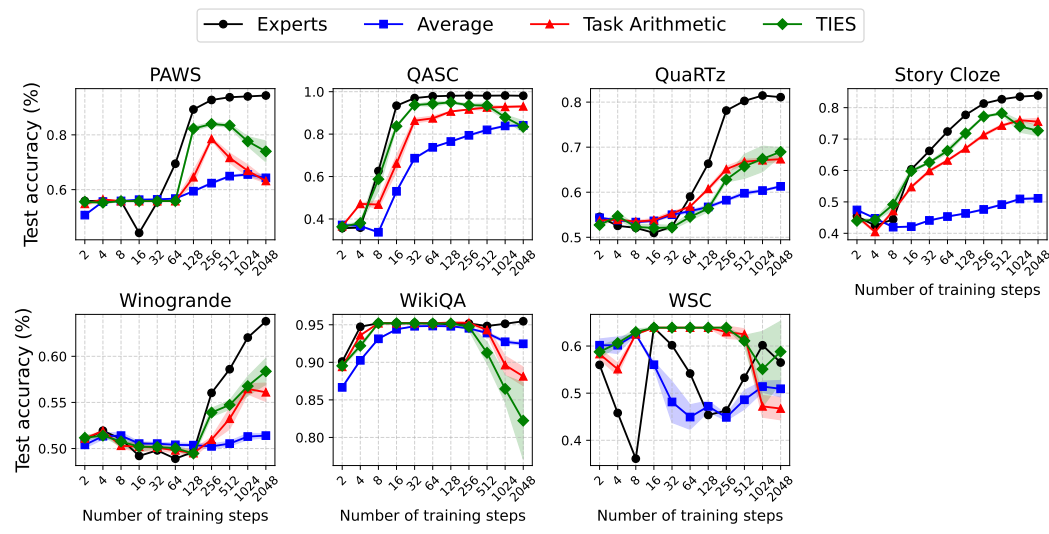
932 Comparing the “useless” 100% from Case 1 with the “useful” 94.4% from Case 2 is meaningless.
933 Absolute, un-normalized accuracy on the other hand allows for a fair and interpretable comparison
934 of the final upcycled model’s quality across different expert training durations.
935
936
937
938
939
940
941
942
943
944
945
946
947
948
949
950
951
952
953
954
955
956
957
958
959
960
961
962
963
964
965
966
967
968
969
970
971

972 D PER-TASK BREAKDOWN OF EXPERT AND MERGING ACCURACIES
973

974 Here we present per-task accuracy plots for the expert and merged models in both the vision (Figure 5) and NLP settings (Figure 6). While there is some variability to the magnitude of the overtraining
975 effect across datasets and merging methods, the direction of the effect is fairly consistent: for
976 most tasks and merging methods, experts trained for significantly fewer steps yield higher merging
977 accuracy. Importantly, we do not rely on any single dataset or outlier task to support our conclusions:
978 the phenomenon is robust across tasks, domains, and merging methods.
979



998 Figure 5: Per-task breakdown of expert and merging accuracies for our ViT-B-32 models trained on
999 8 image classification tasks. Mean and standard deviation across 3 random seeds shown.
1000



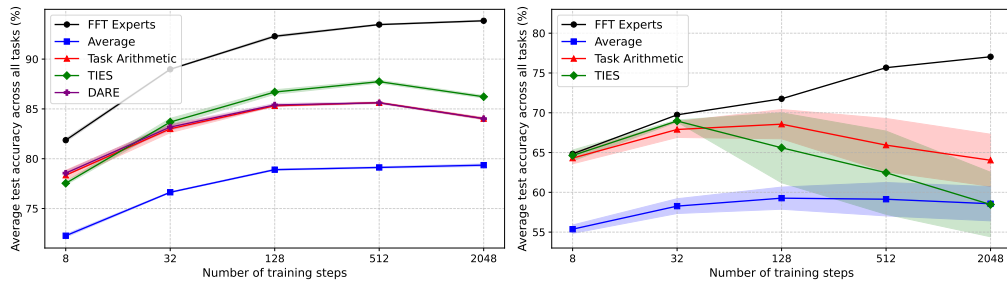
1019 Figure 6: Per-task breakdown of expert and merging accuracies for our T5 models trained on NLP
1020 tasks. Mean and standard deviation across 3 random seeds shown.
1021
1022
1023
1024
1025

1026 E RESULTS WITH ADDITIONAL MODELS

1028 To further reinforce the generality of our results, we have also run experiments with other model
 1029 architectures.

1031 E.1 VISION - ViT-L-14

1033 In the vision setting we have fine-tuned CLIP (Radford et al., 2021) ViT-L-14 (Dosovitskiy et al.,
 1034 2021) models on the same set of 8 image classification tasks introduced in Section 2. We used
 1035 the same training hyper-parameters as for the ViT-B-32 models. The results are shown in Figure 7.
 1036 The same phenomenon can be observed for the larger ViT-L-14 models, while the average expert
 1037 accuracy keeps increasing throughout training, the average merging accuracy peaks early in training.
 1038 Task Arithmetic reaches a peak accuracy of 85.6% at 512 steps before decreasing to 84.0% at 2048
 1039 steps. TIES reaches a peak accuracy of 87.7% at 512 steps of training before decreasing to 86.2%
 1040 at 2048 steps. DARE also peaks at 512 steps with an average accuracy of 85.6% before decreasing
 1041 to 84.0% at 2048 steps. Lastly, Average merging again seems more robust to the negative effects
 1042 of overtraining on model merging, as in our main results. It continues improving with training
 1043 reaching a peak accuracy of 79.4% at 2048 steps, only slightly better than the 79.1% achieved at
 1044 512 steps. However Average merging yields significantly worse results than all other considered
 1045 methods, regardless of the number of fine-tuning steps.



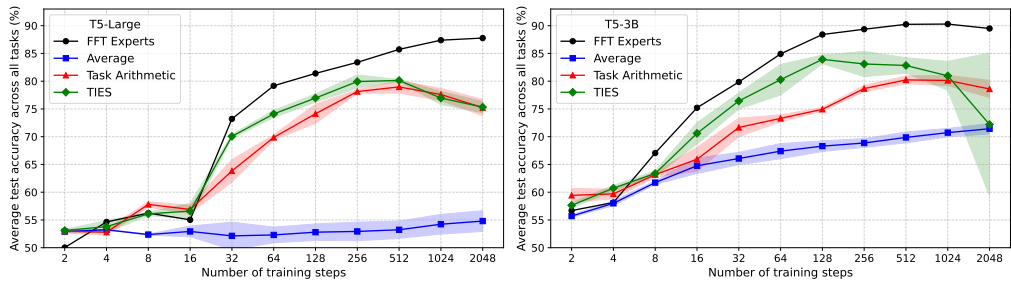
1055 Figure 7: **(left)** Average test accuracy across all 8 vision tasks for fully fine-tuned ViT-L-14 models.
 1056 **(right)** Average test accuracy across all 7 NLP tasks for fully fine-tuned BERT base models. We
 1057 plot the average accuracy of the expert models evaluated on their respective tasks as well as merging
 1058 accuracies for multiple methods. Shaded regions show mean \pm std over 3 random seeds.

1060 E.2 NLP - BERT BASE

1062 In the NLP setting we have fine-tuned BERT base (Devlin et al., 2019) language models on the same
 1063 set of 7 natural language processing tasks introduced in Section 2. For training we used a constant
 1064 learning rate of 2e-5, the remaining hyper-parameters being the same as for the T5 models. The
 1065 results are shown in Figure 7. The same phenomenon can be observed for the BERT models, while
 1066 the average expert accuracy keeps increasing throughout training, the average merging accuracy
 1067 peaks early in training. TIES reaches a peak accuracy of 69.0% at only 32 steps of training before
 1068 decreasing to 58.5% at 2048 steps. Task Arithmetic reaches a peak accuracy of 68.6% at 128 steps
 1069 before decreasing to 64.0% at 2048 steps. Lastly, even Average merging which seemed more robust
 1070 to the negative effects of overtraining on model merging reaches a peak accuracy of 59.3% at 128
 1071 steps before decreasing to 58.6% at 2048 steps.

1080 F EFFECT OF MODEL SCALE
1081

1082 In the right panel of Figure 2, we have investigated how model size influences the merging dynamics
1083 by comparing Task Arithmetic merging results across T5-Base (220M parameters), T5-Large
1084 (770M), and T5-3B (3B). In Figure 8 we also show the average expert accuracy on their respec-
1085 tive tasks as well as the merging accuracies for Average, Task Arithmetic and TIES methods. The
1086 purpose of these experiments is to test whether the decrease in merging accuracy observed after ex-
1087 tended fine-tuning in smaller models also occurs at larger scales. We find that the same phenomenon
1088 persists: for both Task Arithmetic and TIES, merging accuracy peaks at an intermediate number of
1089 training steps and then degrades as fine-tuning continues, even though the absolute merging accu-
1090 racy is generally higher for the larger models. Interestingly, Average merging appears robust to this
1091 degradation, but its overall accuracy remains comparatively low.



1102 Figure 8: Average test accuracy across all 7 NLP tasks for fully fine-tuned T5-Large (**left**) and T5-
1103 3B (**right**) models. We plot the average accuracy of the expert models evaluated on their respective
1104 tasks as well as merging accuracies for multiple methods. Shaded regions show mean \pm std over 3
1105 random seeds.

1106 G EFFECT OF LORA RANK
1107

1109 In this section, we examine how the choice of LoRA rank affects the degradation effect reported in
1110 the main paper. We find that increasing the LoRA rank mitigates the loss in merging accuracy that
1111 occurs as experts are trained for longer.

1112 We fine-tune ViT-B-32 models on the eight image-classification tasks from Sec-
1113 tion 2.5, applying LoRA adapters to every linear layer while systematically varying
1114 the adapter rank r . We employ square-root scaling for the LoRA factor α , choosing
1115 $(r, \alpha) \in \{(16, 45), (32, 64), (64, 90), (128, 128), (256, 181)\}$. The models are trained for
1116 varying number of steps $s \in \{8, 32, 128, 512, 2048\}$ to assess how training duration interacts with
1117 rank. When merging, we combine LoRA-adapted models with the same rank and trained for the
1118 same number of steps. The resulting accuracies are plotted in Figure 9.

1119 Across all three merging methods (Average, Task Arithmetic, and TIES) increasing the LoRA
1120 adapter rank consistently raises merging accuracy at every training duration. Moreover, higher
1121 ranks substantially attenuate the accuracy drop associated with extended training: as the number
1122 of fine-tuning steps grows, models with larger ranks exhibit smaller declines from their peak merg-
1123 ing performance.

1124
1125
1126
1127
1128
1129
1130
1131
1132
1133

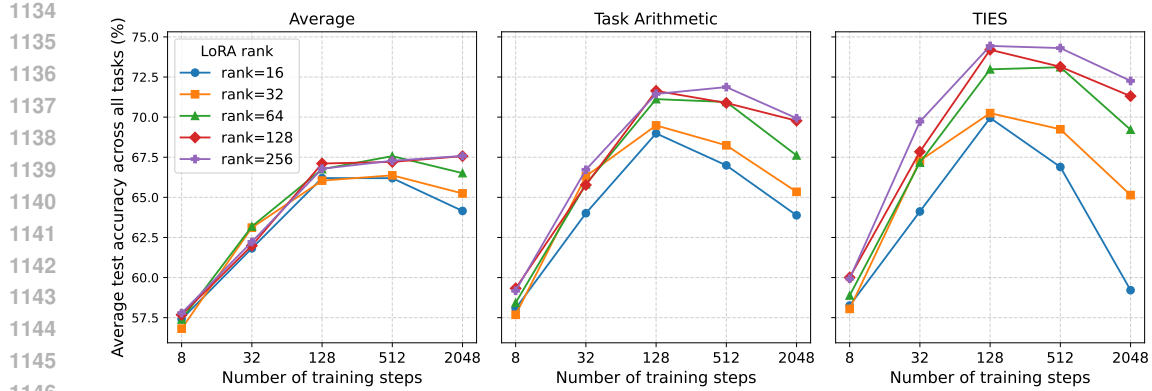


Figure 9: Average test accuracy across all 8 vision classification tasks as a function of the number of fine-tuning steps for different LoRA ranks and three merging methods. Each panel shows one method: Average (left), Task Arithmetic (center) and TIES (right). Colored solid lines and distinct markers denote the different LoRA adapter ranks. The x-axis is in \log_2 scale.

H MEMORIZATION ANALYSIS OF EARLY VS. LATE CHECKPOINTS

A central hypothesis in our work is that *longer finetuning drives models to increasingly memorize difficult training examples*. To test this, we compare CLIP ViT-B-32 models trained for **256** steps (“early”) to models trained for **2048** steps (“late”) across eight image classification datasets (Cars, DTD, EuroSAT, GTSRB, MNIST, RESISC45, SUN397, SVHN) with three random seeds each. Although both checkpoints show high training accuracy overall (100% on easy examples at both stages; 75.1% \rightarrow 95.6% on hard examples from 256 to 2048 steps), memorization manifests not primarily in raw accuracy but in the *trajectory of prediction confidence, loss, and probability distributions*. We show that while accuracy on hard examples improves by 20.5 percentage points, the underlying memorization metrics exhibit changes that are *orders of magnitude* larger relative to easy examples, revealing the mechanism by which extended training drives memorization.

To quantify this, we compute three per-example metrics designed to detect late-stage memorization effects. All metrics are computed on the training set, and then aggregated into 10 difficulty bins per dataset using EL2N scores (Section 4). Each dataset is partitioned into 10 quantile-based bins, where bin 1 contains the easiest 10% of examples and bin 10 contains the hardest 10%. To prevent large datasets from dominating the averages, all results are first aggregated *per dataset* and then averaged across datasets (mean-of-means). For a training example with label y at training step $t \in \{256, 2048\}$, we denote the predicted probability vector as $p^{(t)} = \text{softmax}(z^{(t)})$ where $z^{(t)}$ are the logits.

H.1 MEMORIZATION METRICS

Change in margin: $\Delta m = m^{(2048)} - m^{(256)}$ where $m^{(t)} = p_y^{(t)} - \max_{c \neq y} p_c^{(t)}$.

The margin measures the confidence gap between the true class probability and the maximum probability assigned to any other class. A strong positive relationship between Δm and difficulty indicates that the late model becomes disproportionately confident on hard examples.

Change in loss: $\Delta \ell = \ell^{(256)} - \ell^{(2048)}$ where $\ell^{(t)} = -\log p_y^{(t)}$.

This measures the drop in cross-entropy loss from early to late training. Large positive values indicate that the late model “forces down” the loss of examples that earlier checkpoints still struggled with, even when the top-1 prediction was already correct.

Predictive distribution shift: $\text{shift} = \|p^{(2048)} - p^{(256)}\|_1$.

This L_1 distance quantifies how much the model’s entire probability vector changes between checkpoints. Large shifts indicate substantial changes to the decision function, revealing targeted late-stage adjustments even when accuracy is unchanged.

1188 H.2 RESULTS
1189

1190 Table 4 summarizes the mean values of each metric for the easiest (bin 1) and hardest (bin 10) exam-
1191 ples, averaged across all datasets and seeds. All three metrics display a strong positive correlation
1192 with difficulty bin number, indicating that additional training preferentially modifies the predictions
1193 of the hardest examples.

| Metric | Easy (bin 1) | Hard (bin 10) | Ratio (Hard/Easy) |
|----------------------------|--------------|---------------|-------------------|
| Δm (margin) | 0.0016 | 0.3911 | 244.6 |
| $\Delta \ell$ (loss) | 0.0009 | 0.5924 | 653.5 |
| Predictive shift (L_1) | 0.0039 | 0.5003 | 129.4 |

1200 Table 4: Per-bin memorization indicators averaged across datasets and seeds. Hard examples ex-
1201 hibit dramatically larger changes between the 256- and 2048-step models, consistent with late-stage
1202 memorization.

1204 H.3 ANALYSIS
1205

1206 All three metrics exhibit a strong, monotonic increase across the 10 difficulty bins (Pearson corre-
1207 lations between bin number and per-bin metric values: Δm : $r=0.914$ ($p=0.0002$), $\Delta \ell$: $r=0.820$
1208 ($p=0.004$), predictive shift: $r=0.920$ ($p=0.0002$)). These highly significant correlations demon-
1209 strate that difficulty bin systematically predicts the magnitude of model changes during extended
1210 training, ruling out random variation as an explanation. This pattern reveals a coherent story:

- 1212 • **Confidence increases (margin)** for hard examples are more than two orders of magni-
1213 tude larger than for easy examples (244.6 \times). Easy examples already achieve near-maximal
1214 margins at 256 steps ($m \approx 0.997$), leaving little room for improvement, while hard exam-
1215 ples undergo substantial margin increases ($\Delta m = 0.39$) as the model learns to confidently
1216 classify them.
- 1217 • **Loss reductions** from 256 to 2048 steps show the most extreme differential effect
1218 (653.5 \times), indicating that extended training “forces” difficult examples into the correct class
1219 by dramatically reducing their cross-entropy loss, even when the top-1 prediction was al-
1220 ready correct at the earlier checkpoint.
- 1221 • **Probability distributions** shift substantially more for difficult examples (129.4 \times), sug-
1222 gesting targeted late-stage adjustments to the decision function. While easy examples
1223 maintain stable predictions (L_1 shift ≈ 0.004), hard examples experience large redistri-
1224 butions of probability mass across classes (L_1 shift ≈ 0.50).

1225 Together, these metrics provide consistent and quantitative evidence that longer finetuning causes
1226 the model to memorize difficult examples: the 2048-step models exhibit large, difficulty-dependent
1227 changes to losses, margins, and probability distributions that are absent or minimal in the 256-step
1228 models. These memorization patterns have important implications for task vector composition and
1229 model merging. Models at different training stages have encoded fundamentally different solutions
1230 to the same classification task: early models rely on generalizable features that work across many
1231 examples, while late models additionally employ example-specific adjustments that memorize indi-
1232 vidual difficult cases. When such heterogeneous models are combined via task arithmetic or model
1233 merging, the interaction between generalizable and memorized components can produce unexpected
1234 emergent behaviors, potentially explaining performance variability in multi-task and few-shot trans-
1235 fer settings.

1236
1237
1238
1239
1240
1241

1242 I QUANTIFYING PARAMETER INTERFERENCE THROUGHOUT TRAINING

1244 **Task Vector Construction** For each dataset d and training step t , we compute a task vector τ_d^t as
 1245 the parameter difference between the fine-tuned model and the pre-trained (zero-shot) model:

$$1247 \quad \tau_d^t = \theta_d^t - \theta_0 \quad (3)$$

1248 where θ_d^t represents the parameters of the model fine-tuned on dataset d for t steps, and θ_0 represents
 1249 the pre-trained model parameters. All floating-point parameters are concatenated into a single vector
 1250 of dimension n .

1252 **Top- $k\%$ Pruning** For analysis, we apply magnitude-based pruning to the task vectors to retain
 1253 only the most significant parameter changes. For a given task vector τ and pruning threshold $k\%$,
 1254 we define the pruned task vector:

$$1256 \quad \tilde{\tau}_i = \begin{cases} \tau_i & \text{if } |\tau_i| \geq \text{threshold}_k \\ 1257 0 & \text{otherwise} \end{cases} \quad (4)$$

1258 where threshold_k is the k -th percentile of $|\tau|$. Unless otherwise specified, we use $k = 20\%$ (retaining
 1259 the top 20% of parameters by absolute magnitude), following the best practice from Yadav et al.
 1260 (2023).

1262 I.1 METRIC DEFINITIONS

1264 **Sign Conflict Percentage.** For each dataset pair (d_1, d_2) , we count the proportion of parameters
 1265 where the task vectors have opposite signs. Let $\mathcal{A} = \{i : \tilde{\tau}_{d_1,i} \neq 0 \vee \tilde{\tau}_{d_2,i} \neq 0\}$ be the set of active
 1266 parameters, and $\mathcal{C} = \{i \in \mathcal{A} : (\tilde{\tau}_{d_1,i} > 0 \wedge \tilde{\tau}_{d_2,i} < 0) \vee (\tilde{\tau}_{d_1,i} < 0 \wedge \tilde{\tau}_{d_2,i} > 0)\}$ be the set of
 1267 parameters with conflicting signs. Then:

$$1269 \quad \text{SignConflict}(d_1, d_2) = \frac{|\mathcal{C}|}{|\mathcal{A}|} \times 100 \quad (5)$$

1271 High sign conflict indicates destructive interference when averaging task vectors.

1273 **Parameter Overlap Percentage** We measure how much the important parameters (top- $k\%$ by
 1274 magnitude) overlap between datasets. For each dataset d , let $\mathcal{M}_d = \{i : |\tau_{d,i}| \geq \text{threshold}_k\}$ be the
 1275 set of important parameter indices. The overlap between two datasets is:

$$1277 \quad \text{Overlap}(d_1, d_2) = \frac{|\mathcal{M}_{d_1} \cap \mathcal{M}_{d_2}|}{|\mathcal{M}_{d_1}|} \times 100 \quad (6)$$

1279 High overlap indicates that different tasks compete for the same parameters, increasing the potential
 1280 for interference during merging.

1282 **Magnitude Ratio** For parameters that are important in both task vectors (i.e., in the overlapping
 1283 set $\mathcal{O} = \mathcal{M}_{d_1} \cap \mathcal{M}_{d_2}$), we measure the disagreement in their magnitudes:

$$1285 \quad \text{MagRatio}(d_1, d_2) = \frac{1}{|\mathcal{O}|} \sum_{i \in \mathcal{O}} \frac{\max(|\tau_{d_1,i}|, |\tau_{d_2,i}|)}{\min(|\tau_{d_1,i}|, |\tau_{d_2,i}|)} \quad (7)$$

1287 A magnitude ratio significantly greater than 1 indicates that even when tasks modify the same pa-
 1288 rameters, they disagree substantially on the extent of modification, leading to interference when
 1289 averaged.

1291 **Per-Parameter Variance** Unlike the pairwise metrics above, per-parameter variance captures
 1292 multi-task disagreement. For each parameter position i , we compute the variance of its changes
 1293 across all D datasets:

$$1295 \quad \text{Var}(i) = \frac{1}{D} \sum_{d=1}^D (\tilde{\tau}_{d,i})^2 \quad (8)$$

1296 where we assume the mean is centered at zero (the pre-trained model). The overall variance metric
 1297 is:

$$1298 \text{Variance} = \frac{1}{|\mathcal{A}_{\text{all}}|} \sum_{i \in \mathcal{A}_{\text{all}}} \text{Var}(i) \quad (9)$$

1300 where $\mathcal{A}_{\text{all}} = \bigcup_{d=1}^D \{i : \tilde{\tau}_{d,i} \neq 0\}$ is the union of all active parameters across datasets. Higher
 1301 variance indicates greater disagreement about how each parameter should be modified, leading to
 1302 information loss during averaging.

1304 I.2 RESULTS

1306 We analyze ViT-B-32 checkpoints trained on the 8 considered vision datasets (Cars, DTD, EuroSAT,
 1307 GTSRB, MNIST, RESISC45, SUN397, SVHN) across 6 training step counts (4, 16, 64, 256, 512,
 1308 2048) and 3 random seeds.

1309 For pairwise metrics (Sign Conflict, Parameter Overlap, Magnitude Ratio), we:

- 1311 1. Compute the metric for all $\binom{8}{2} = 28$ dataset pairs at each step and seed
- 1312 2. Average across the 28 pairs to obtain a single value per step per seed
- 1313 3. Compute the mean and standard deviation across the 3 seeds

1316 For the per-parameter variance metric, we:

- 1317 1. Compute variance across all 8 datasets simultaneously at each step and seed
- 1318 2. Compute the mean and standard deviation across the 3 seeds

1320 The results are presented in Table 5 and Figure 10.

1322 Table 5: Parameter interference metrics across training steps (mean \pm std across 3 seeds). Metrics
 1323 computed on the union of each dataset’s top 20% parameters by magnitude.

| 1325 Steps | 1326 Sign Conflict (%) | 1327 Param Overlap (%) | 1328 Mag Ratio | 1329 Variance |
|------------|------------------------|------------------------|----------------------|--|
| 1327 4 | 1328 7.24 ± 0.03 | 1329 26.09 ± 0.07 | 1330 1.03 ± 0.00 | 1331 $(1.35 \pm 0.00) \times 10^{-10}$ |
| 1328 16 | 1329 7.20 ± 0.01 | 1330 26.46 ± 0.02 | 1331 1.23 ± 0.00 | 1332 $(1.06 \pm 0.00) \times 10^{-9}$ |
| 1329 64 | 1330 7.42 ± 0.01 | 1331 27.67 ± 0.00 | 1332 1.38 ± 0.00 | 1333 $(4.05 \pm 0.01) \times 10^{-9}$ |
| 1330 256 | 1331 7.77 ± 0.01 | 1332 28.75 ± 0.02 | 1333 1.43 ± 0.00 | 1334 $(1.27 \pm 0.01) \times 10^{-8}$ |
| 1331 512 | 1332 7.92 ± 0.01 | 1333 29.08 ± 0.02 | 1334 1.43 ± 0.00 | 1335 $(2.37 \pm 0.01) \times 10^{-8}$ |
| 1332 2048 | 1333 8.03 ± 0.00 | 1334 29.53 ± 0.01 | 1335 1.48 ± 0.01 | 1336 $(8.15 \pm 0.04) \times 10^{-8}$ |

1333 Table 5 presents parameter interference metrics across training steps, revealing systematic increases
 1334 in all interference measures as training progresses. Sign conflict percentage increases modestly from
 1335 7.24% to 8.03%, indicating a slight rise in parameters with opposing signs across tasks. Parameter
 1336 overlap grows from 26.09% to 29.53%, showing that longer training causes different tasks to
 1337 increasingly compete for the same important parameters. The magnitude ratio increases from 1.03 to
 1338 1.48, demonstrating growing disagreement about the extent of parameter modifications even when
 1339 tasks modify the same parameters in the same direction. Most dramatically, per-parameter variance
 1340 increases by approximately 60-fold from 1.35×10^{-10} to 8.15×10^{-8} , providing strong evidence
 1341 that extended training causes datasets to diverge substantially in their parameter modifications. Col-
 1342 lectively, these metrics demonstrate that longer training amplifies parameter interference, directly
 1343 explaining the degradation in merge performance observed with increased training steps. The con-
 1344 sistency of these trends across all metrics and the low standard deviations across seeds indicate that
 1345 this phenomenon is robust and reproducible.

1346
 1347
 1348
 1349

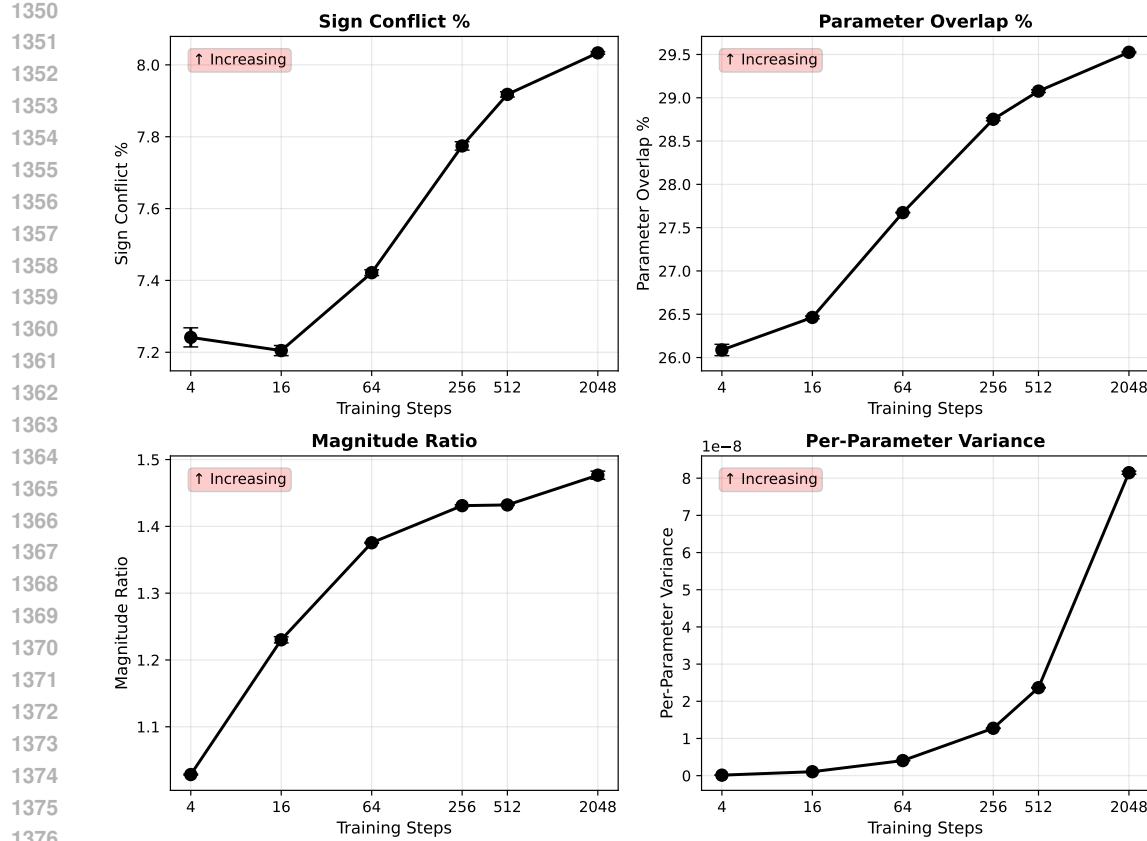


Figure 10: Parameter interference metrics across training steps (mean \pm std across 3 seeds). Metrics computed on the union of each dataset’s top 20% parameters by magnitude.

J PSEUDOCODE FOR THE ViT EARLY STOPPING STRATEGY

Here we provide pseudocode for the LR scheduler and early stopping strategy with linear warm-up and adaptive decay used for ViT models.

1404
1405
1406
1407
1408
1409
1410
1411
1412
1413
1414
1415
1416
1417
1418

Algorithm 1: Early stopping strategy with linear warm-up and adaptive decay

Input: Peak LR η_{\max} , warm-up steps $S_{\text{warm}}=50$, validation interval $S_{\text{val}}=5$, patience $P=3$, decay factor $\gamma=0.5$, minimum LR threshold $\eta_{\min} = 1e-7$

Initialize learning rate $\eta=0$, best validation accuracy $A_{\text{best}}=0$, plateau counter $c=0$

for training step $s = 1, 2, \dots$ **do**

```

1424 if  $s \leq S_{\text{warm}}$  then
1425    $\eta \leftarrow \eta_{\text{max}} \cdot \frac{s}{S_{\text{warm}}}$                                 // Linear warm-up
1426
1427 else
1428   // Adaptive decay and early stopping
1429   if  $s \bmod S_{\text{val}} = 0$  then
1430     Evaluate validation accuracy  $A_{\text{val}}$ 
1431     if  $A_{\text{val}} > A_{\text{best}}$  then
1432        $A_{\text{best}} \leftarrow A_{\text{val}}$ 
1433        $c \leftarrow 0$ 
1434     else
1435        $c \leftarrow c + 1$ 
1436     if  $c \geq P$  then
1437        $\eta \leftarrow \gamma \cdot \eta$ 
1438        $c \leftarrow 0$ 
1439     if  $\eta < \eta_{\text{min}}$  then
1440       stop training
1441
1442 Update model parameters using  $\eta$ 

```

1443
1444
1445
1446
1447
1448
1449
1450
1451
1452
1453
1454
1455
1456
1457